Norwegian University of Life Sciences

Master's Thesis 2021 60 ECTS
Faculty of Chemistry, Biotechnology and Food science

The Role of HCAR1 on Oligodendrocyte Proliferation and Survival after Neonatal Hypoxia Ischemia in Mice

Marie Landa Austbø
Master of Science, Biotechnology

The Role of HCAR1 on Oligodendrocyte Proliferation and Survival after Neonatal Hypoxia Ischemia in Mice

Oslo University Hospital, Rikshospitalet, Department of Microbiology,

and

The Norwegian University of Life Sciences, Faculty of Chemistry, Biotechnology and Food Science

Acknowledgement

The work of this thesis was carried out at the Department of Microbiology at Oslo University Hospital (OUS) from August 2020 to May 2021, as part of a master's degree in Biotechnology at the Norwegian University of Life Sciences (NMBU).

First and foremost, I would like to thank my supervisor Johanne Egge Rinholm for giving me the opportunity to participate in this exciting project and for introducing me to the field of neuroscience. Thanks for all supervision, support, and enthusiasm throughout the year, and thanks for always being available for guidance in the laboratory and in the process of writing this thesis. I would also like to thank my internal supervisor Harald Carlsen at NMBU, for practical help and guidance with this thesis.

A special thanks to PhD student Emilie Rylund Glesaaen, who has been there to help me through the entirety of this project. Thanks for your help in the laboratory, excellent guidance, and support. I would also like to thank the rest of the Rinholm group; Niklas Meyer, Britina Kjuul Danielsen and Ali Al-Jabri for providing a lively and including working atmosphere.

Thanks to Prof. Stefan Offermanns and collaborators at the Max-Planck-Institute for Heart and Lung Research, Bad Nauheim, Germany, for providing breeder HCAR1 knockout mice, and Raji Suganthan for assistance with hypoxic-ischemic experiments. Thanks to Arne Klungland, Magnar Bjørås, Linda Bergersen, Pierre Chymkowitch and Lauritz Kennedy for their helpful collaborations that made the presented work possible. Images were obtained with support from Anna Lång and Stig-Ove Bøe at the South-Eastern Health Authority Core Facility of Advanced Light Microscopy.

Lastly, I would like to thank my fellow students in the student’s office, Britina Kjuul Danielsen and Xiaoxiong Ma. I have greatly appreciated the company, and friendship throughout the year.

Oslo, May 2021

Marie Landa Austbø

Abstract

Neonatal cerebral hypoxia-ischemia (HI) is a leading cause of death and disability in infants. It is characterized by insufficient supply of blood and oxygen to the brain, resulting in cell death and tissue loss. The only current treatment of neonatal HI is hypothermia, a treatment that is only effective for moderate HI insults, and not beneficial for more than 30% of surviving babies. In addition, many of the survivors still experience long-term neurological effects such as cerebral palsy, epilepsy, and cognitive disabilities. New treatments that can reduce the brain injury and improve tissue regeneration after HI are therefore needed.

The oligodendrocytes and their myelin are highly vulnerable to hypoxia ischemia and other forms of brain injury. Myelin insulates the nerve fibers and is crucial for effective action potential propagation and neuronal health. HI leads to oligodendrocyte death and damage and consequently demyelination of the axons. An important goal for brain tissue repair after injury is therefore to be able to stimulate the production of new oligodendrocytes to remyelinate the axons. Our group and others have previously shown that lactate can support myelination and cell proliferation in the brain, an effect that was attributed to its metabolic properties. New studies suggest that lactate exert some of its protective effects through the newly discovered Hydroxycarboxylic acid receptor 1 (HCAR1), but *in vivo* studies are scarce. The purpose of this study was to investigate whether this lactate receptor is involved in oligodendrocyte survival and proliferation after brain injury, and to find out which cell types express HCAR1 in the mouse brain.

This study revealed HCAR1 expression in oligodendrocytes in the corpus callosum of mouse brain sections. HCAR1 was also detected in the subventricular zone, neocortex, and the granular cell layer of the dentate gyrus of the hippocampus, indicating that HCAR1 is expressed in a variety of other cells. By using a mouse model for cerebral HI, this study showed that mice lacking HCAR1 have a reduced number of proliferated oligodendrocytes after HI compared with wild type (WT) mice. When investigating loss of mature oligodendrocytes however, a similar reduction of oligodendrocytes was detected in both genotypes after injury. These data suggest that HCAR1 is important for oligodendrocyte proliferation, but not oligodendrocyte survival, after HI. In the long term, these findings could contribute to increase our understanding of pathologies that involve cerebral HI and could point to HCAR1 as a therapeutic target for future treatment of these conditions.

Sammendrag

Neonatal hypoksisk iskemi (HI) er en ledende årsak til dødsfall og funksjonsnedsettelser hos nyfødte. Tilstanden kjennetegnes ved utilstrekkelig tilførsel av blod og oksygen til hjernen, som resulterer i celledød og vevstap. Hypotermi er per dags dato den eneste behandlingsmetoden for HI hos nyfødte. Denne behandlingsmetoden er bare effektiv for moderate tilfeller av HI og en betydelig andel av de barna som overlever får senskader som cerebral parese, epilepsi samt kognitive funksjonsnedsettelser. Det er derfor et behov for nye behandlingsmetoder som kan redusere hjerneskaden samt fremme vevsregenerering etter HI.

Oligodendrocyttene og deres myelin er svært sårbare for HI og andre former for hjerneskade. Myelinet som dannes av oligodendrocyttene beskytter og isolerer nervefibrene, og er helt avgjørende for effektiv signaloverføring i hjernen. HI fører til at oligodendrocyttene blir skadet og dør, og dermed til demyelinisering av aksoner. Etter en hjerneskade slik som HI er det derfor viktig for hjernen å kunne stimulere produksjonen av nye oligodendrocytter for å remyelinisere aksonene. Vår gruppe og andre har tidligere vist at laktat kan bidra til myelinisering og celleproliferasjon i hjernen. Tidligere trodde man at alle de positive effektene av laktat skyldtes laktat som metabolitt, men nye studier tyder på at noen av de beskyttende effektene til laktat går via den nylig oppdagede hydroksykarboksylsyre-reseptor 1 (HCAR1), men mer forskning trengs på dette området. Hensikten med denne studien var å undersøke om denne laktatreseptoren er involvert i oligodendrocytt-overlevelse samt proliferasjon etter hjerneskade. Vi ønsket også å finne ut hvilke celletyper i musehjernen som utrykker HCAR1.

Denne studien avdekket ved hjelp av musehjernesnitt at HCAR1 utrykkes i oligodendrocytter i hjernebjelken. HCAR1-utrykk ble også påvist i den subventrikulære sonen, i hjernebarken samt i hippocampus, noe som tyder på at HCAR1 utrykkes i flere celletyper i hjernen. Ved å bruke en musemodell for HI, viste denne studien at mus som mangler HCAR1 har et redusert antall prolifererte oligodendrocytter etter hjerneskade sammenlignet med villtype-mus. Undersøkelsen av tap av modne oligodendrocytter viste derimot en lignende reduksjon av oligodendrocytter i begge genotypene etter hjerneskade. Disse dataene antyder at HCAR1 er viktig for oligodendrocytt-proliferering, men ikke for oligodendrocytt-overlevelse etter HI. På lang sikt kan disse funnene bidra til å øke vår forståelse av patologier som involverer HI og kan peke på HCAR1 som et terapeutisk mål for fremtidig behandling av disse tilstandene.

Abbreviations

APC	Adenomatous polyposis coli
ATP	Adenosine triphosphate
BrdU	5-bromo-2'-deoxyuridine
BSA	Bovine serum albumin
cAMP	Cyclic adenosine monophosphate
CCA	Common carotid artery
cDNA	Complementary DNA
CLSM	Confocal laser scanning microscopy
CNS	Central nervous system
Ctrl	Control
Cq	Quantitation cycle
DAPI	4′,6-diamidino-2-phenylindole
DG	Dantate gyrus
df	Degrees of freedom
dsDNA	Double stranded DNA
EtOH	Ethanol
FACS	Fluorescence-activated cell sorting
FISH	Fluorescent in situ hybridization
GAPDH	Glyceraldehyde 3-phosphate dehydrogenase
GLUT	Glucose transporter protein
GPCR	G-protein-coupled receptor
GPR81	G-protein receptor 81
h	Hour
HCAR	Hydroxycarboxylic acid receptor
HCAR1	Hydroxycarboxylic acid receptor 1
HRP	Horseradish peroxidase
HI	Hypoxia-ischemia
IHC	Immunohistochemistry
KO	Knock-out

Lac	Lactate
MCT	Monocarboxylate transporter
MQ-H_2O	Milli-Q water
mRFP	Monomeric red fluorescent protein
mRNA	Messenger RNA
NA	Numeric aperture
NADH	Nicotinamide adenine dinucleotide
NBF	Neutral Buffered Formalin
OL	Oligodendrocyte
Olig2	Oligodendrocyte transcription factor 2
OPC	Oligodendrocyte precursor cell
P(n)	Postnatal day (n=number)
PBS	Phosphate buffered saline
PBS-T	Phosphate buffered saline-Tween
PCR	Polymerase chain reaction
PFA	Paraformaldehyde
PKA	Protein kinase A
PVDF	polyvinylidene fluoride
RNA	Ribonucleic acid
RT-qPCR	Quantitative reverse transcription polymerase chain reaction
qPCR	Quantitative Polymerase chain reaction
RNase	Ribonuclease
RT buffer	Reverse transcription buffer
SD	Standard deviation
SDS-PAGE	Sodium dodecyl sulphate-polyacrylamide gel electrophorese
SEM	Standard error of mean
ssDNA	Single stranded DNA
SVZ	Subventricular zone
TSA	Tyramide Signal Amplification
V	Volt
WT	Wild type

TABLE OF CONTENTS

1. Introduction

The introduction will contain information that can be of use when reading this thesis. First a brief introduction of the brain and its cells will be given with focus on the myelinating cells of the central nervous system, the oligodendrocytes. Then the pathological condition cerebral hypoxia ischemia will be presented, and it will be described how this condition affects the oligodendrocytes. Lactate as an energy substrate and a signalling molecule will be described, and the newly discovered lactate receptor in the brain, HCAR1 will be presented. Finally, animal experiments and the ethics around the use of animal models in research will be described.

1.1 The brain

The brain is one of the largest and most complex organs in the human body. It consists of the cerebrum, cerebellum, and the brain stem and together with the spinal cord makes up the human central nervous system (CNS). The neurons are the most characteristic cells of the CNS, primarily responsible for information transfer. The neurons are crucial, but they depend on, interact with, and are surrounded by other cells that are important for proper brain function, the glial cells. Astrocytes, microglia, and oligodendrocytes are all glial cells that support the neurons in different ways. Astrocytes are key homeostatic controllers of the CNS and play an important role in information transfer in neuronal networks (1). Microglia act as phagocytes and are called the immune cells of the brain (2). The last type of glial cells is the oligodendrocytes (OL). Oligodendrocytes are the myelin producing cells in the CNS and will be described in detail in the next paragraphs.

1.2 Oligodendrocytes: the myelin producing cells

The largest part of the brain, cerebrum, consist of two types of tissue termed white and grey matter. The white matter is characterized by bundles of myelinated axons connecting the neurons in the grey matter (3). Myelin is a membranous, lipid rich substance that wraps around and insulates axons, allowing for efficient propagation of action potentials. The beginning of myelin biology can be traced back to 1717 when Leeuwenhoek described “nervules” surrounded by “fatty parts” (4). The name myelin from Greek *myelos* after bone marrow colour and texture was later given by German pathologist Rudolf Ludwig Virchow in 1854 (5). Science waited almost 250 years after myelin first was described before it was demonstrated that these fatty parts could be traced to an oligodendrocyte (6-9). Since then, it has become well known that oligodendrocytes myelinate

axons in the CNS, and that the insulating properties of myelin increase the conduction velocity of the action potential.

One oligodendrocyte can myelinate multiple axons. This contrasts with the myelinating cells in the peripheral nervous system, the Schwann cells, which only myelinate one axon each. Myelin is an extension of the membrane of the myelinating cell. The membrane wraps around the axon in multiple layers held together by anchoring proteins, making a compact structure called myelin sheaths. The myelin sheaths provide a thick electrical insulation, which allows nerve impulses to move at a much higher speed than in non-myelinated axons due to a phenomenon called saltatory conduction. Multiple myelin sheaths (internodes) enfold the axons, only interrupted by short unmyelinated areas dense in ion channels called nodes of Ranvier (illustrated in figure 1.1). Upon an action potential, the electrical impulse will "jump" from one node of Ranvier to the next whereas ions can flow into the axon, hence the name saltatory conduction by the Latin word *saltare*, "to leap" (10). The electrical insulation inhibits depolarization of the cellular membrane and without myelin, the axons would need to be so large that it would not be compatible with our anatomy (11).

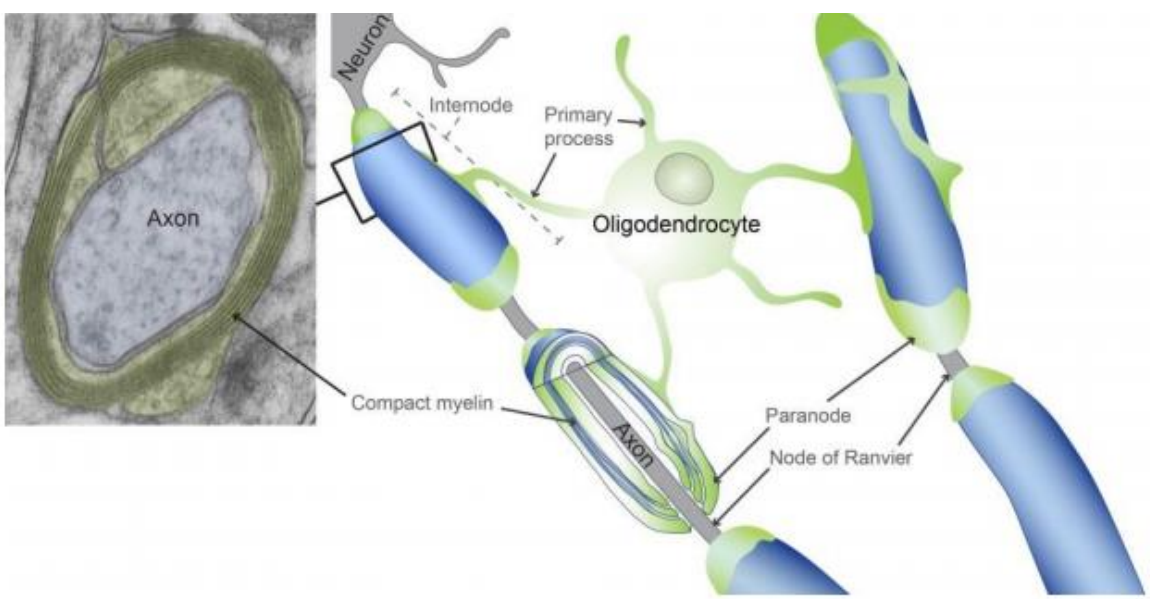

Figure 1.1. Illustration of an oligodendrocyte myelinating two axons. The image shows the myelin sheaths (internodes), the compact myelin with the multi layering of membrane around the axon (an electron micrograph of a cross-section of a myelinated axon) and nodes of Ranvier. Adapted from Rinholm et al. 2016 (12).

1.2.1 From OPC to Oligodendrocyte

All oligodendrocytes start as oligodendrocyte progenitor cells (OPC). The OPCs arise from neuroectodermal stem cells in the ventricular zone during early development, further they proliferate and migrate to different areas of the brain where they terminally differentiate into mature oligodendrocytes that myelinate axons (13). Unlike other progenitor cells the OPCs persist throughout life, they are self-renewing and can differentiate into mature OLs to maintain myelin plasticity or in response to damaging signals (14). The differentiation from OPC into a mature and myelinating oligodendrocyte can be divided into four stages: OPC, late OPC, premyelinating oligodendrocyte and myelinating oligodendrocyte (illustrated in figure 1.2) (15). The differentiation process is tightly controlled by activation and repression of specific growth and transcription factors (16). As these transcription factors regulate OPC proliferation, migration, and differentiation they can serve as stage-specific cell markers of the oligodendrocyte cell linage. One of these transcription factors is the oligodendrocyte transcription factor 2 (Olig2) which is expressed in all stages of the OL cell linage and can thus serve as a general marker for all OPCs and OLs (17). Another marker is adenomatous polyposis coli (APC), a tumour suppressor gene detected in cell bodies of mature oligodendrocytes that can be used as a marker to detect pre- and myelinating oligodendrocytes (18).

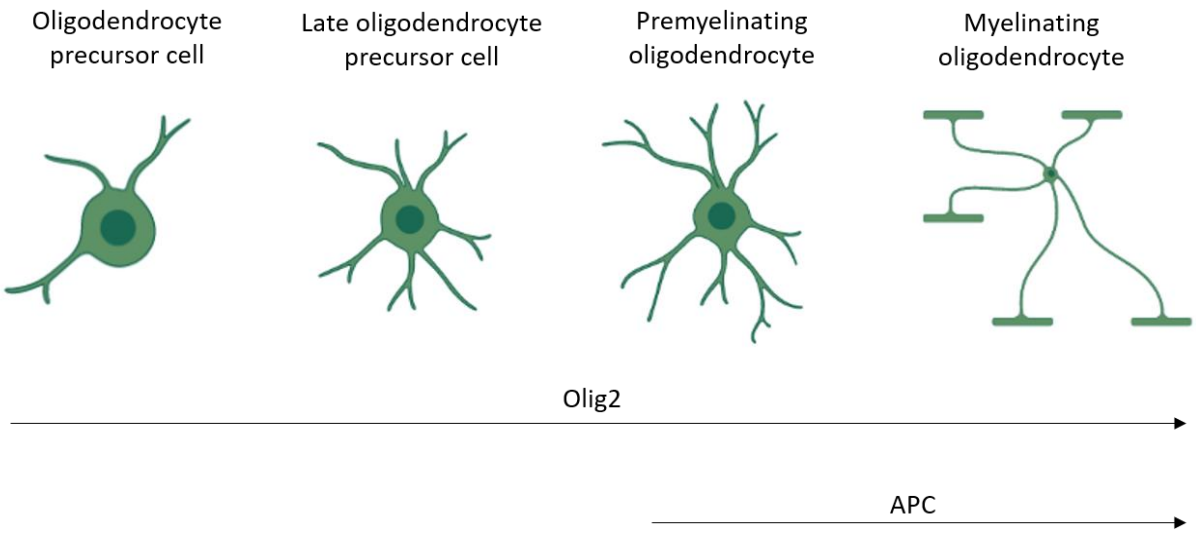

Figure 1.2. Illustration of the oligodendrocyte cell linage. The differentiation from oligodendrocyte precursor cell (OPC) into a myelinating oligodendrocyte can be divided into four stages: OPC, late OPC, premyelinating oligodendrocyte, and myelinating oligodendrocyte. The transcription factor Olig2 is expressed in all stages of the oligodendrocyte cell linage. APC is expressed in pre- and myelinating oligodendrocytes. Created in BioRender.com

1.3 Neonatal cerebral hypoxia ischaemia

Neonatal cerebral hypoxia-ischemia (HI) is the leading cause of death and disability in newborns and affect around 1.5 per 1000 live born births in the developed countries (19). HI can occur as result of multiple conditions such as heart disease, lung malformations, problems with blood flow to the placenta, drug or alcohol abuse and preeclampsia. Common for all these conditions are that they result in impaired cerebral blood flow and oxygen delivery to the brain during or around the time of birth. The deprivation of oxygen and blood to the developing brain leads to cell death and brain tissue damage and thus have devastating consequences for the newborn.

The only current treatment of neonatal hypoxia-ischemia is hypothermia, in which the head or the whole body is cooled down to lower the body temperature. However, this treatment is only effective for moderate HI insults, and is not beneficial for more than 30% of surviving babies (20-22). In addition many of the survivors still experience long-term neurological effects such as cerebral palsy, epilepsy and cognitive disabilities (23).

1.3.1 The effect of HI on oligodendrocytes

After an episode of cerebral hypoxia-ischemia, early events include overactivation of glutamate and adenosine triphosphate (ATP) receptors, oxidative stress, and inflammation (24). Oligodendrocytes are unfortunately very vulnerable to such conditions and are acutely damaged by short periods of HI. As early as 30 minutes post arterial occlusion cell swelling occurs, and it is shown that after 3 hours, large numbers of oligodendrocytes are lethally injured (25). A consequence of oligodendrocyte death and damage is demyelination and dysmyelination, resulting in loss of the axonal insulation and eventually neuronal failure. In response to a demyelination event a remyelination process is activated where new myelinating oligodendrocytes are generated from early postnatal-derived OPCs present in the brain (26). The OPCs are recruited to the damaged area where they start to proliferate, migrate, and populate the demyelinated area. The recruited OPCs start to differentiate into mature myelinating oligodendrocytes that form myelin sheaths around the demyelinated axons (27).

Loss of myelinating oligodendrocytes and OPCs is also associated with a variety of other pathological conditions such as Multiple sclerosis, Alzheimer's disease, and Huntington's disease (28-31). Given that the oligodendrocytes and myelin are susceptible to multiple diseases and injury

conditions, a deeper understanding of the mechanisms responsible for their death and replacement with new remyelinating oligodendrocytes is essential (32).

The myelin may not be limited to function solely as an insulator that speeds up the action potentials by enabling saltatory conduction. Recent studies have shown that the myelin sheaths provide metabolic support to the axons in the form of lactate (33-35). Furthermore, the oligodendrocytes seem to be very vulnerable to low energy conditions during myelination of the axons, and may consume lactate for energy production and for lipid synthesis (36, 37).

1.4 Lactate

Lactate was first discovered in sour milk in 1780 by the Swedish chemist, Scheele (38), and was for a long time after its discovery regarded as a sheer waste product of metabolism (39, 40). However, the concept of lactate as just metabolic leftover product has been challenged in recent times by new ideas and studies of muscles and brain metabolism (41-44). It is now known that lactate is a major energy source, major gluconeogenic precursor as well as a signalling molecule in the brain (45). Two enantiomers of lactate exist, due to the presence of a chiral carbon. The two isoforms are known as L-lactate and D-lactate, with L-Lactate being the most abundant and physiological significant isoform in mammalian cells (46). From here on the term lactate refers to L-Lactate.

1.4.1 Lactate fuels brain cells

Glucose is the primary energy source in the adult brain (47), but lactate has shown to be an important energy source before and immediately after birth, because the glucose level in the blood is low at this time, whereas the lactate level is high (48). Glucose enters the cell through glucose transporter proteins (GLUTs). Inside the cell cytoplasm, glucose is broken down via glycolysis to generate two three-carbon sugars of pyruvate. The conversion of glucose to pyruvate produces a small amount of ATP and nicotinamide adenine dinucleotide (NADH) for the cell to use for energy. Pyruvate can further diffuse into mitochondria and enter the Krebs cycle and oxidative phosphorylation, which generates a large amount of energy in the form of ATP (49). Pyruvate can also have a different fate following glycolysis. Instead of entering the mitochondria the cytosolic enzyme lactate dehydrogenase converts pyruvate to lactate, and lactate is exported out of the cell. Lactate is then imported by other cells where it is converted back to pyruvate and further metabolized in mitochondria (illustrated in figure 1.3).

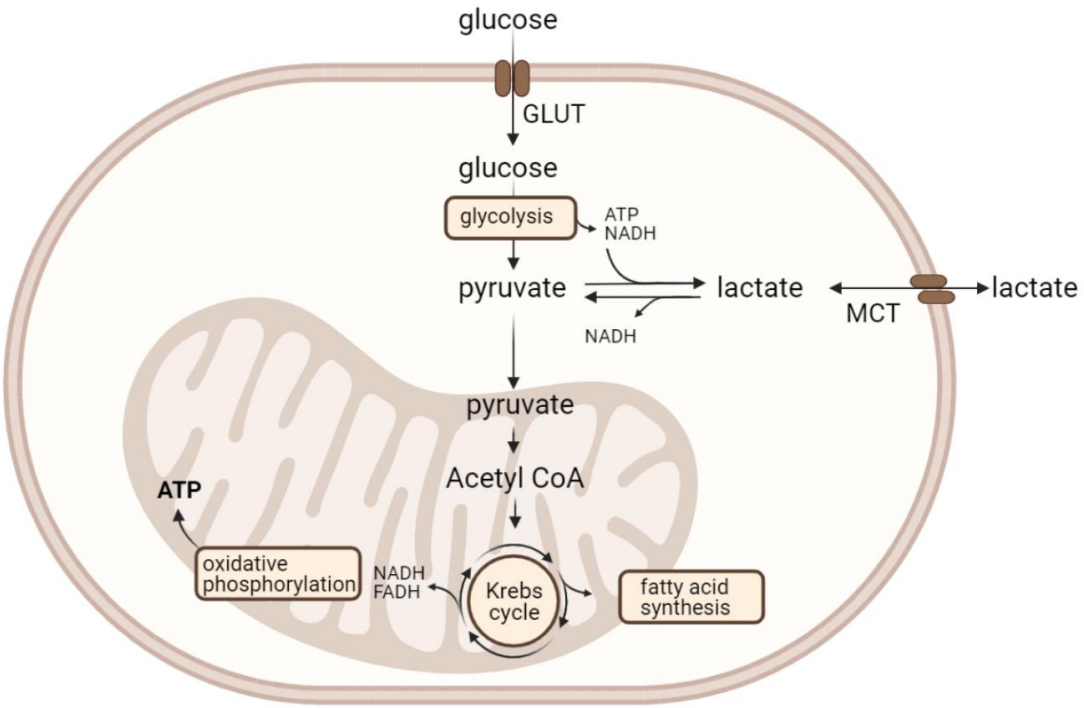

Figure 1.3. Schematic drawing of cerebral glucose and lactate metabolism. Glucose enters the cells through glucose transporters (GLUTs) and is broken down to pyruvate through ATP producing glycolysis. Pyruvate can diffuse into mitochondria and enter the Krebs cycle and oxidative phosphorylation, which generates a large amount of ATP. Pyruvate can also convert to lactate with the enzyme lactate dehydrogenase. Lactate is transported across cell membranes by monocarboxylate transporters (MCT). Created in BioRender.com

1.4.2 Lactate transporters

Monocarboxylate transporters (MCTs) are responsible for transporting lactate across cell membranes. Fourteen MCT subtypes have been identified of which MCT1-4 have shown to catalyse a proton-coupled transport of lactate and other monocarboxylates (50-55). MCT4 was recently reported on astrocytes, which have high glycolytic activity and the ability to supply lactate to other brain cells (56, 57). MCT2 is found in the cell bodies, dendrites and axons of neurons with the main task of importing lactate (56-59). The most abundant subtype of the monocarboxylate transporters is MCT1 (60). MCT1 is reported on endothelial cells lining the capillary walls, transporting lactate across the blood brain barrier (56, 61). MCT1 was also recently found in oligodendrocytes as well as myelin sheaths (34, 37). Studies have shown that oligodendrocytes supply lactate to the neurons alongside the astrocytes, and consume lactate to rescue myelination during hypoglycaemia (33, 34, 37, 62).

1.4.3 Lactate support myelination

At the peak of myelination, it is estimated that oligodendrocytes synthesize an amount of lipid equal to 3 times their cell body weight (63). At this point the need for substrates to support lipid synthesis is highly increased. Developing oligodendrocytes have shown to take up and consume lactate both in brain slices (37), and in primary cultures (36) from mice. Beside aiding lipid synthesis lactate has also shown to be important in the acetylation of histones which is important for oligodendrocyte differentiation and myelination (64). As previously described oligodendrocytes are very vulnerable to energy deprivation (see 1.3.1 The effect of HI on oligodendrocytes). Lack of energy can limit the availability of carbon substrates and ATP for the synthesis of myelin lipids, thus oligodendrocytes may require alternative substrates such as lactate for survival. Our group previously showed that organotypic brain slices cultured in low glucose resulted in loss of oligodendrocytes as well as myelination, but by supplying lactate this loss could be prevented (37). Lee et al. also showed that lactate released from oligodendrocytes and myelin is crucial for axon health. They showed this by knockdown of MCT1 expression in oligodendrocytes which led to abnormal axon morphology and neuronal death (in animal and cell culture models) that could be prevented by supplying lactate (34). Recent studies in mice have also shown improved recovery after neonatal HI by administration of lactate (21, 65).

1.4.4 Lactate as signalling molecule

Signalling molecules are responsible for transmitting information between cells in multicellular organisms. These molecules show enormous variation in their structure as well as function and range from simple gases to amino acids, carbohydrates, lipids, and proteins. Despite their variation all signalling molecules act as a ligand for receptors expressed by their target cell (66). Recent studies in various tissues and cell types under physiological and pathological conditions now suggest that lactate should be considered as an important signalling molecule and not just a metabolic end product (67-69). The Hydroxycarboxylic acid receptor 1 (HCAR1) was recently discovered in the brain, giving a possible route for lactate signalling in the central nervous system (70). The positive effects of lactate have for a long time been limited to its ability to provide metabolic support to cells. With the new discovery of the lactate receptor it is now questioned if some of these effects could be a result from signalling via HCAR1.

1.5 Lactate receptor HCAR1

The Hydroxycarboxylic acid receptor 1 (HCAR1, also known as HCA1 or GPR81) is a seven transmembrane G-protein-coupled receptor (GPCR). The GPCRs are the most abundant of all receptor families in eukaryote organisms, they play an essential role in physiology and disease and numerous GPCRs are targets of important drugs in use today (71). In fact, more than 60% of all currently prescribed drugs act on GPCRs, making them the most important target for pharmacological therapies (72). The GPCRs consist of seven transmembrane helices bound to a G-protein. There are three types of G-proteins, G_i, G_q, and G_s which upon ligand-binding and receptor activation changes confirmation and interact with ion channels and enzymes, and thereby act on various intracellular pathways.

HCAR1 was first discovered in 2001. At this time the ligand of the receptor was unknown, and thus it was classified as an orphan GPCR and named G-protein receptor 81 (GPR81) (73). The receptor was in 2009 shown to be activated by the metabolite 2-hydroxypropanoate (lactate) and later given the name hydroxycarboxylic acid receptor 1 (74). HCAR1 is a part of a GPCR subfamily consisting of receptors activated by hydroxycarboxylic acid ligands. The two other receptors in this family are HCAR2 and HCAR3 activated by β-Hydroxybutyric acid and 3-Hydroxyoctanoic acid respectively (75, 76). The three hydroxycarboxylic acid receptors are all located closely together in the genome and share high sequence homology with each other (73). HCAR1 and HCAR2 are found in most mammalian species while HCAR3 expression is restricted to higher primates (77). All HCARs are expressed in adipose tissues where they have shown to inhibit lipolysis and are thought to play a role in regulating lipid metabolism. The hydroxy-carboxylic receptors are also expressed in other organs such as liver, spleen, kidney and skeletal muscles (74, 78-81).

Lauritzen et al. recently discovered HCAR1 in widespread regions of the brain, concentrated on postsynaptic membranes as well as vascular endothelial membranes (70). HCAR1 is activated by lactate, its activation leads to G_i-dependent inhibition of adenylyl cyclase, which decreases intracellular cyclic adenosine monophosphate (cAMP) and consequently protein kinase A (PKA) levels (illustrated in figure 1.5) (82). HCAR1 activation has shown to modulate neuronal firing rates *in vitro* and to stimulate brain angiogenesis *in vivo* (82, 83). Recently our group showed that mice lacking the lactate receptor have a reduced ability to regenerate brain tissue after HI (84).

Examination of neurosphere cultures *in vitro* and immunohistochemical staining of brain tissue after HI showed that HCAR1 knockout (KO) mice display impaired proliferation of neuronal progenitor cells as well as microglia. Microglia were also less activated in the KO mice (84). Studies from different cell lines such as breast cancer cells and osteoblasts also suggest that HCAR1 may regulate cell proliferation and differentiation (85). Thus, HCAR1 could be targeted to promote tissue repair after HI, but its role in the brain remains to be further investigated.

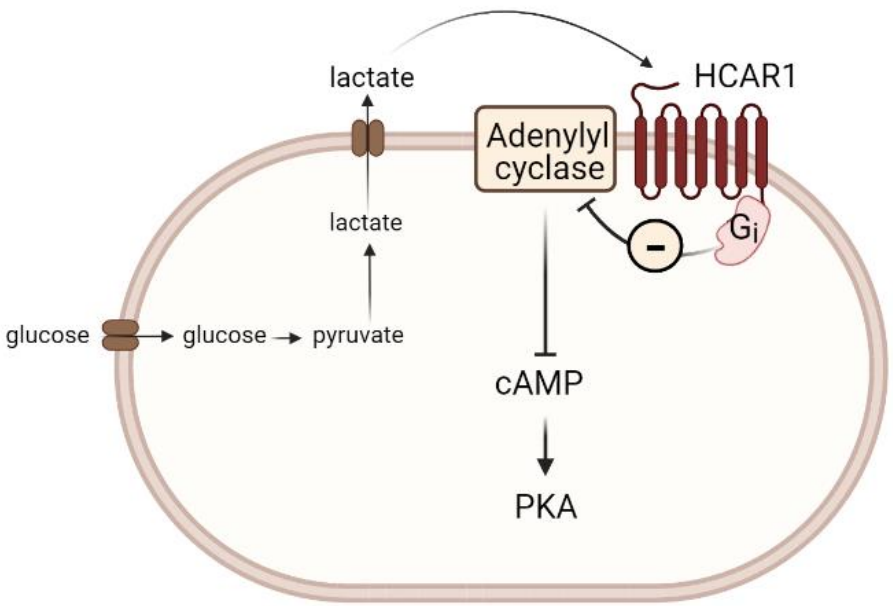

Figure 1.5. Schematic drawing of the physiological function of the HCAR1 receptor. Glucose enters the cell and is broken down to pyruvate which is converted to lactate. Lactate activates HCAR1 receptors and decreases intracellular cAMP and consequently PKA levels through G_i-dependent inhibition of adenylyl cyclase. Created in BioRender.com.

1.6 Animal experiments and ethics

1.6.1 Animal selection

Animal models of ischemic stroke serve as an essential tool first to investigate the mechanisms of ischemic brain injury and secondly for the development of better prevention and treatment strategies. Most of our knowledge on the pathophysiological mechanisms involved in cerebral ischemia comes from animal studies most often carried out in small animals such as rats and mice. The use of small animals for stroke research studies present clear advantages over larger animals; they are less expensive, more suitable for ischemic surgery and genetic modification, and are more

ethically acceptable (86, 87). It is important to notice that mimicking all aspects of human hypoxia ischemia in one animal model is impossible, since HI is a very heterogeneous disorder. Thus, the use of an animal model does not attempt to model the whole disease process but rather aims to enable detailed study of specific aspects of the disease in controlled circumstances.

1.6.3 Differences between human and animal models

Using an animal model has its limitations, although the rodents show similarities in cerebrovascular anatomy and pathophysiology there are also important differences compared to humans. The human brain is much bigger than in rodents, they differ in length and structure of perforating arteries, and the ratio of grey to white matter is substantially lower in humans. Mice have a grey to white matter ratio of 90:10, while the human brain has a ratio of 40:60 (87). Reflecting this difference in grey to white matter, mouse brain also differs in the glial to neuron ratio compared to the human brain. Studies done on primates and humans suggest an evolutionary escalating glial to neuron ratio, indicating that the human brain is comprised of a much higher percentage of glial cells than the mouse brain (87, 88). This might reflect why several pharmacological agents have been effective in animal models but not in humans (89).

1.6.4 Ethics and experiments on animals

Over the past century animal research has had a vital role in many scientific and medical advances and continues to aid our understanding of various diseases. The human life quality is improved due to these advances and development of new medicines and treatments is possible due to animal research (90). However, the ethical assessments related to the use of animals in research are wide-ranging. While it is generally thought that it may be necessary to use laboratory animals to create improvements for people, animals or the environment, it is at the same time a general opinion that animals have a moral status, and that our treatment of them should be subject to ethical considerations (91). The use of animals in neurobiological research is a prerequisite to obtain a deeper understanding of the human brain, even though cell cultures and computer models could replace some animal experiments. More knowledge is also necessary if we want to improve the treatment for diseases affecting the central nervous system. Such diseases have devastating consequences and as if today the treatments are limited. Current neurobiological research is promising but it depends on animal experiments to test the hypotheses. Even though it is considered ethically justifiably to use animals in neurobiological research there are strict rules considering which ones that are allowed to perform animal experiments, and how it is done in

order to reduce the discomfort and pain to a minimum. For example, all procedures must be conducted under full anaesthesia. In Norway, the use of laboratory animals is governed by the Regulations Relating to the Use of Animals in Research, which follow from the Animal Welfare Act (2, 91).

2. Aim of study

The myelin sheath around nerve fibers is crucial for effective action potential propagation and neuronal health. Myelin is a specialized extended membrane produced by oligodendrocytes. Unfortunately, oligodendrocytes and their myelin are highly vulnerable to brain ischemia and other forms of brain injury. An important goal for brain tissue repair after injury is therefore to be able to stimulate the production of new myelin. Our group has previously shown that lactate can support myelination and cell proliferation in the brain. However, it is unclear whether this is a pure metabolic effect of lactate or dependent on the newly discovered lactate receptor (HCAR1). **The aim of this thesis is to investigate whether the lactate receptor is involved in oligodendrocyte survival and proliferation after neonatal cerebral hypoxia ischemia. We also want to find out which cell types express HCAR1 in the mouse brain.**

3. Materials and methods

3.1 Experimental setup

4 experimental setups were used to help achieve the aims of this study. A brief overview is presented with text and illustrations (Figure 3.1) underneath.

1. **To test whether HCAR1 plays a role in oligodendrocyte survival and proliferation after hypoxia ischemia.**

   Method: Perfusion fixation with paraformaldehyde of HCAR1 knock-out and wild type mice combined with immunohistochemistry and confocal microscopy.

2. **Investigate the protein level of oligodendrocyte markers.**

   Method: Protein extraction followed by sodium dodecyl sulphate-polyacrylamide gel electrophorese (SDS-PAGE) and western blot on striatum samples from HCAR1 KO and WT mice

3. **Investigate the RNA expression of oligodendrocytes and HCAR1.**

   Method: Quantitative reverse transcription polymerase chain reaction (RT-qPCR) of brain tissue from HCAR1 KO and WT mice.

4. **Detection and localization of HCAR1 in the mouse brain.**

   Method: Perfusion fixation with paraformaldehyde of WT mice combined with RNA fluorescent in situ hybridization (RNA-FISH), immunohistochemistry and confocal microscopy.

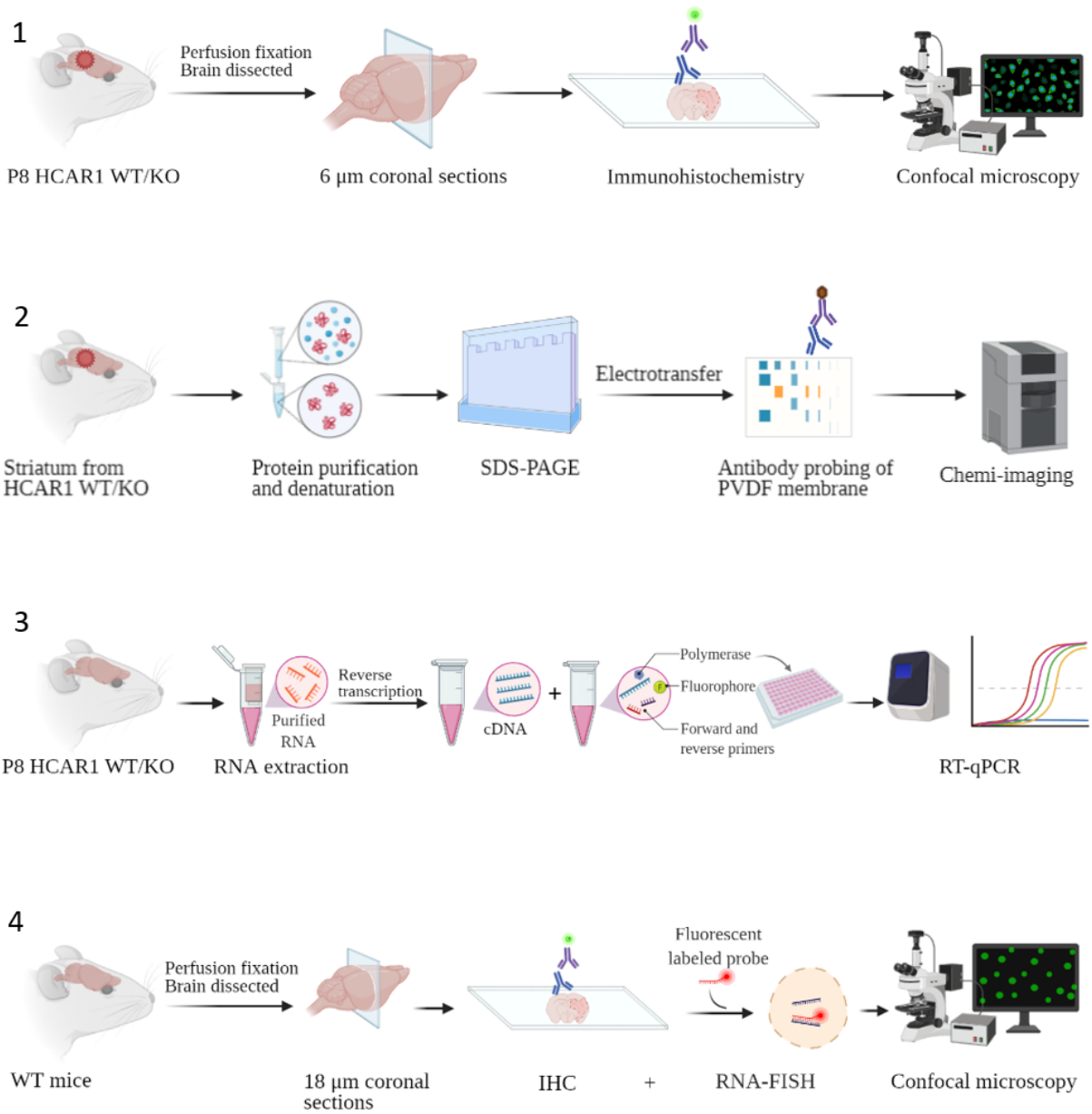

Figure 3.1. Illustration of the methods used in this study. Illustration of the methods used for this study. 1: Immunohistochemistry, 2: Western blot, 3: Quantitative reverse transcription polymerase chain reaction, 4: RNA fluorescent in situ hybridization combined with immunohistochemistry. Created in BioRender.com.

All reagents, kits, consumables, instruments, and software that have been used in this study are listed in Appendix, section A, with producers, and catalogue numbers. Solutions and buffers used in this study are listed in appendix, section B.

3.2 Animals

For this study transgenic HCAR1 knock-out (KO) and C57BL/6N wild type (WT) mice were used. The HCAR1 KO line was obtained from Prof. Dr Stefan Offermanns, Max Planck Institute for Heart and Lung Research, Bad Nauheim, Germany. Homologous recombination in embryonic stem cells was used to inhibit the expression of the HCAR1 receptor. This inhibition was done by exchanging the exon encoding HCAR1 with a cassette encoding β-galactosidase (LacZ) and neomycin-resistance. C57BL/6N mice were bred with the HCAR1 KO, and genotypes were determined by polymerase chain reaction (PCR) analysis of DNA samples extracted from mouse ears (83). In this study homozygote mice were used, HCAR1 -/- (KO) and HCAR1+/+(WT). Mice at postnatal day 8 (P8) were used for the experiments, and both sexes are represented. All mice had free access to rodent food and water, and they were housed in a climate-controlled environment on a 12h light/dark cycle. The mice were treated in accordance with national ethical guidelines (Norwegian Animal Welfare Act and European Communities Council, Directive of 24. November 1986-86/609/EEC) and kept at the Oslo University Hospital's Department of Comparative Medicine. All experimental procedures were approved by the Norwegian Animal Research Authority and were conducted by FELASA-certified operators.

3.3 Mouse model for cerebral HI

Permanent occlusion of the left common carotid artery (CCA) followed by systemic hypoxia was used to produce cerebral hypoxia and ischemia (HI) in P8 mice, as previously described (92). This was done by a technician as follows: P8 mice were anaesthetized with isoflurane (4% induction in chamber, 2,5% maintenance on mask in a 2:1 mixture of ambient air and oxygen). A skin incision was made in the interior midline of the neck, the left CCA was exposed and separated from adjacent tissue. A monopolar cauterizer (Hyfrecator 2000; ConMed) at 4.0 watt was used to electro coagulate the artery by placing a needle in the CCA. Absorbable sutures (Safil 8-0 DRM6; B. Braun Melsungen AG) was used to close the neck incision, and the whole surgical procedure was completed within 5 minutes. Following the surgical procedure, the P8 mice had a recovery period of 1-2 hours before they were exposed to a hypoxic (10% oxygen balance nitrogen, Yara), humidified atmosphere for 60 min at 36 ºC. This model for HI leads to a central zone of irreversibly damaged tissue (ischaemic core) confined to the brain hemisphere ipsilateral to the occluded CCA, whereas the contralateral hemisphere is indistinguishable from a sham-treated brain and is used in this study as a morphologically accurate internal control (92).

At 7 days post HI, the brains were dissected out and prepared for immunohistochemistry. The mouse brains used in mRNA and protein analysis were dissected out 6 hours post HI.

3.4 Preparation of mouse tissue for microscopic study

A good preparation of the animal tissue is important for high quality results in a microscopic study. The tissue must be treated carefully so that their structure can readily be visualized under the microscope. It is also important that the tissue is as little altered as possible in the process in order to obtain a view of their basic structure comparable to that of living state (93).

3.4.1 Tissue processing

Fixation is the first step in tissue processing and is essential for good results. The goal of fixation is to prevent decomposition, putrefaction, and autolysis while preserving the tissue as close to its natural form as possible (94). Small pieces of tissue can be fixed by immersion fixation, in which the tissue is placed directly in a fixative that disperses through the sample. The immersion technique works poorly on larger specimens like the brain as the fixative has problem reaching all the tissue at the same rate. The penetration distance is too large and thus the core of the brain will be exposed to less fixative than the periphery (95).

For the IHC and FISH experiments it was important that the brains were evenly fixed, and as we study hypoxia it was important to keep the brains from a hypoxic environment. Therefore, perfusion fixation (*in vivo* fixation), which uses the circulation system of the animal to evenly distribute the fixative was considered the best method (96). The perfusion fixation was done by a technician. In this method a needle is inserted into the ventricle, pumping a fixative into the systemic circuit. The fixative can by this method quickly reach all parts of the organism by travelling through the vascular system (96). Paraformaldehyde (PFA) was the fixative used in this study. PFA is a polymer composed of four units of formaldehyde that quickly penetrates the tissue and conserves the cytoarchitecture by creating methylene bridges (CH_2-cross-links) between nitrogen and proteins in the tissue (97). In this study, mice were first anesthetized with a cocktail consisting of Zoletil Forte (Virbac international, Carros Cedex, France), Rompun (Bayer Animal Health GmbH, Leverkusen, Germany) and Leptanal (Janssen-Cilag International NV, Beerse, Belgium), then 4% PFA was pumped through the left ventricle by a peristaltic pump (7-8 ml/min).

The brains used for IHC experiments were fixed by 4% PFA *in vivo*, then dissected out and stored in 4% PFA for 24 h, and then immersion fixed in 10% formalin until paraffin embedding. For

RNA-FISH, the brains were perfused *in vivo* with 4% PFA, dissected out and stored in 4% PFA for 24 h before immediately proceeding with cryopreservation. Perfusion fixation does not allow for the study of brain biochemistry. The brain tissue that was used for the protein and mRNA analyzes was therefore fresh-frozen and stored at -80°C to preserve DNA, RNA, and proteins.

3.4.2 BrdU incorporation in mice

To investigate the regeneration of oligodendrocytes after hypoxia ischemia 0.1 mg/g 5-bromo-2'-deoxyuridine (BrdU) was injected by a technician into the mice at day 4 to 7 after HI at 24h intervals. BrdU is a thymidine analogue that incorporates DNA of dividing cells during the S-phase of the cell cycle. As such, BrdU can be used for monitoring cell proliferation (98). The mice used in this study were transcardially perfused 2h after the last BrdU injection as described above.

3.5 Immunohistochemistry

Coons et al. marked the beginning of immunohistochemistry (IHC) in 1942 with a publication describing an immunofluorescence technique for detecting cellular antigens in tissue sections (99). Since then, IHC has been improved to become a valuable tool in both diagnosis and research by combining three scientific disciplines: immunology, histology, and chemistry (100). IHC is based on the binding of antibodies to specific antigens in the tissue. Antibodies are produced by the immune system in vertebrates and work as a defence against infection. The antibodies are made in different forms, each with a different binding site that recognizes a specific antigen. This precise antigen specificity of antibodies is utilized in immunostaining and makes it possible to detect specific molecules in the tissue. By labelling the antibodies with fluorescent dyes, specific molecules can be detected in cells by fluorescent microscopy.

Immunohistochemistry can either be done directly or indirectly. In direct IHC the fluorescent dye is linked directly to an antibody used for specific recognition, the primary antibody. Indirect IHC is used in this study, a method that uses both the primary antibody as well as secondary antibodies to get a stronger signal. The primary antibody is unlabelled and binds to the wanted antigen, while the secondary antibody is labelled with a fluorescent dye and is specific for the host organism where the primary antibody is made. The labelled secondary antibody binds the primary antibody-antigen and the signal can be detected in a microscope (illustrated in figure 3.2) (101). Despite being more time consuming than the direct method, the indirect method is much more sensitive as

the detected signal is amplified by binding of multiple secondary antibodies to the primary antibody (102).

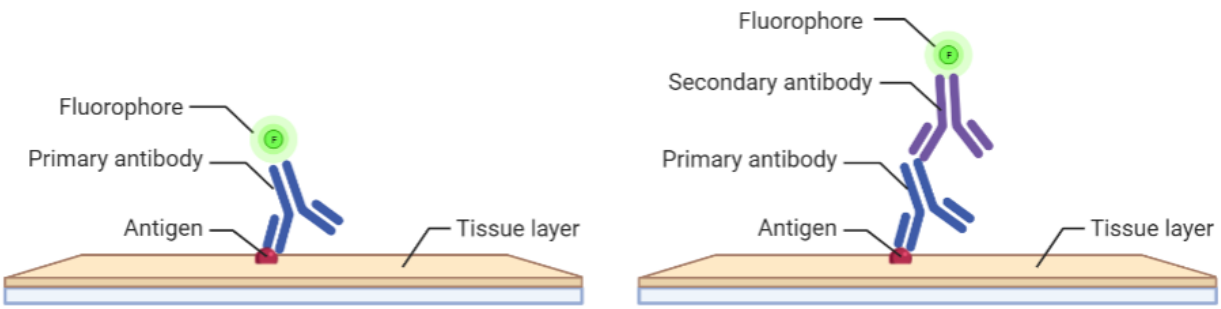

Figure 3.2 Illustration of direct and indirect immunohistochemistry (IHC). The first image illustrates direct IHC: Primary antibody with attached fluorophore binds the target antigen on the tissue layer. Second image illustrates indirect IHC: Primary antibody binds the target antigen. A secondary antibody with an attached fluorophore, binds the primary antibody-antigen. Created in BioRender.com.

3.5.1 Protocol for fluorescence immunostaining of paraffin sections.

Paraffin embedding was used for IHC experiments as this method is thought to better preserve morphological details and allows for thinner sections and thus good microscopic resolution (102). A microtome (Thermo Fisher Scientific) was used to cut 6 µm-thick sections of the brain. The paraffin sections were cooled on ice prior to sectioning, as cold wax allows thinner sections to be obtained. The temperature of the water bath was 40 °C, below the melting point for paraffin (50-57°C), but high enough so that sections flattened out on the surface of the water. For this study coronal sections were used over sagittal sections. Coronal sectioning was necessary as a comparison of the two hemispheres, affected ipsilateral hemisphere vs. contralateral hemisphere was done for the IHC experiments.

The immunostaining protocol for paraffin sections was performed as follows: Since paraffin sections were used it was important to remove the wax and rehydrate the sections as the staining solutions are aqueous. To solve this, the slides were put in a heating incubator (Termaks) at 60 ºC for 30 minutes to melt off the paraffin. Then the sections were deparaffinized in a fume hood by immersing in Clear Rite (2 x 5 min) followed by rehydration in an alcohol gradient (100% EtOH 2 x 5 min, 96% EtOH 5min and 70% EtOH 5 min) and then transferred to Milli-Q water (MQ H_2O).

After deparaffinization and rehydration the slides were transferred to boiling citrate buffer (pH 6.0) for antigen retrieval in 20 minutes using the coverslip-paperclip method described by Vinod et al (103). After antigen retrieval the slides were left at room temperature to cool down, washed with phosphate-buffered saline (PBS) and dried with tissue paper (kimwipes). A PAP pen (ImmEDGE, Vector Laboratories) was used to encircle the sections. This hydrophobic pen makes a lipophilic barrier around the sections and prevents the antibody solution from floating out during incubation. All the following steps were carried out at room temperature unless otherwise is specified. The slides were placed in a moisture chamber and incubated with blocking solution (10% normal goat serum, 1% bovine serum albumin, 0.5% Triton X-100 in PBS) for 1 hour. Then the sections were incubated with mouse anti-APC (1:100, Abcam), rabbit anti-Olig2 (1:200, Merck Millipore) and rat anti-BrdU (1:200, Abcam) diluted in antibody solution (3% normal goat serum, 1% bovine serum albumin, 0.5% Triton X-100 in PBS) overnight in a moisture chamber.

The next day the sections were washed 3x10 min with PBS and incubated with Alexa Fluor 555 goat anti-mouse (1:400, Invitrogen), Alexa Fluor 488 goat anti-rabbit (1:400, Invitrogen), Alexa Fluor 633 goat anti-rat (1:400, Invitrogen), and 4′,6-diamidino-2-phenylindole (DAPI) (1:5000 Sigma-Aldrich) diluted in antibody solution for 2 h in moisture chamber. Sections were rewashed 3x10 min in PBS and mounted with ProLong™ Glass Antifade Mountant (Thermo Fisher Scientific). Cover glass thickness was 0.13-0.17mm. The cover glass was sealed with nail polish to prevent the sections from drying out and stored in dark at 4 ºC until observation in confocal microscope. After observation the slides were stored long-term at -20 ºC.

3.5.2 Confocal laser scanning microscopy

Confocal microscopy is an imaging technique within fluorescence microscopy invented by Marvin Minsky in 1955 that offers several advantages over conventional widefield optical microscope (104). Unlike the widefield microscopy the confocal laser scanning microscopy (CLSM) is equipped with lasers, pinhole, scanner unit and detector system which improves the resulting images. The illumination source in the confocal consists of lasers which emit light with highly specific wavelengths, thereby increasing the accuracy of fluorochrome excitation. The confocal is also equipped with a pinhole located under the detector system. The pinhole rejects out of focus light as only light from the focal plane of the sample reaches the detector. Instead of illuminating the whole specimen at once as in widefield microscopy, the confocal focuses a spot of light onto a single point at a specific place in the specimen and allows for optical sections from selected

depths. The detectors in the confocal converts the emitted photons into digital images and makes it possible to perform a sequential scan in order to avoid crosstalk of the fluorochromes (105).

For imaging the results of the IHC stained sections a Leica TCS SP8 STED confocal microscope with Leica LASX software was used. The images were taken with a 20x objective (numerical aperture (NA) 0.75) and 40x oil-immersion objective (NA 1.3) Two images from each section were captured in a z-stack of 5. One image was taken in the peri-infarct zone of the affected, ipsilateral side of the brain, and one image of the contralateral side used as control.

3.5.3 Image processing and analysis

All the images in this study were analysed using the ImageJ open-source, Java based imaging program, developed at the National Institute of Health by Wayne Rasband (106). By using ImageJ one can visualize, inspect, quantify, and validate scientific image data. The images uploaded in ImageJ from the confocal microscopy are raster images. A raster image is a type of digital image that uses tiny rectangular pixels, arranged in a grid formation to represent an image. Each pixel in an image contains one or more bits of information, depending on the degree of details. The number of bits in each pixel is known as the colour depth while the number of pixels defines the resolution of an image (107).

ImageJ was in this study used for cell quantification of oligodendrocytes. All oligodendrocytes, mature oligodendrocytes and proliferating oligodendrocytes were quantified. The Z-stacks were flattened with average intensity z-projection before analysing. Manual thresholding was used to create a binary image. Cells were counted with the "Analyze particles" function. Cells were also counted manually on some of the images using the Cell Counter plugin in Fiji Image J to test the accuracy of the algorithms. Olig2+ cells overlapping with DAPI+ cells were counted to quantify oligodendrocytes, a triple overlap with BrdU+ cells were counted to quantify proliferated oligodendrocytes. For quantification of mature oligodendrocytes, a counting of APC+ overlapping with Olig2+ cells were done. The imaging and image analysis were blinded to avoid bias.

3.5.4 Statistical analysis and construction of graphs in Prism

The data obtained in ImageJ were transferred to Microsoft Excel, organized into groups and unblinded. The Šídak (108) method was used for multiple comparison of selected groups: WT-contra vs KO-contra, WT-ipsi vs KO-ipsi, WT-contra vs WT-ipsi and KO-contra vs KO-ipsi. GraphPad Prism was used for statistical analysis and construction of graphs. All results are

presented as mean ± standard error of the mean (SEM). Error bars were not included, as all individual data points are presented in the graphs. Degrees of freedom are written as df in the results. n= number of subjects/mice. All experimental units were included in the analyses (none were excluded).

3.6 Western blot

Western blotting is a technique used to identify specific proteins based on molecular weight from a complex mixture of proteins extracted from cells or tissue. This technique involves the separation of proteins by gel electrophoresis, their transfer to a membrane, and selective immunodetection using specific primary and secondary antibodies (109). Western blotting was used in this study to analyse protein levels of the oligodendrocyte marker Olig2 in striatum samples from P8 HCAR1 KO and WT mice (6h post HI).

3.6.1 Protein extraction and separation

Tissue from the striatum of mouse brains was pulverized in an Eppendorf tube on dry ice with a pellet pestle (Life Sciences). 50µL Lysis buffer containing 1%PIC and 5%DDT was added to the sample and incubated on a rolling incubator (Labinco) at 4°C for 15 minutes. The lysate was then added to pre wet QIAshredder (QIAGEN) and spun down at 16 000 rpm for 1 min x 2 at 4°C. Protein concentrations were determined by the Bradford method (110), using bovine serum albumin (BSA)(Sigma-Aldrich) as a standard. This was important to ensure that the samples were compared on an equivalent basis, i.e. that the same amount of protein was loaded for each sample.

4XNuPAGE® LDS sample buffer (Thermo Fischer Scientific) was added to the sample in a 1:4 concentration. The sample buffer contains glycerol, allowing the samples to easily sink into the wells of the gel, and a tracking dye, allowing us to see how far the separation has progressed. The samples were also heated to 65 °C in the buffer to denature the proteins and make them negatively charged, thus enabling the proteins to move towards the positive electrode when voltage is applied.

Protein extracts were separated by sodium dodecyl sulphate-polyacrylamide gel electrophorese (SDS-PAGE). Samples were loaded on a 12% Mini-PROTEAN® TGX™ Precast Protein Gel (Bio-Rad). 2 µL Precision Plus Protein™ Dual Colour Standard (Bio-Rad) was loaded on the first well, and 10 µL of each protein sample were loaded in the following wells. The gels were run in a XCell SureLock Mini-Cell chamber (Thermo Fisher Scientific) and 1X Tris-Glycine SDS Running

Buffer (Bio-Rad) was used. Proteins were separated at 200 Volt (V) for 30-40 minutes until the front colour of the marker reached the bottom line.

3.6.2 Blotting

A Trans-Blot® Turbo™ Mini PVDF Transfer Pack (Bio-Rad) was used to transfer proteins from the mini gel to a 0.2 µm polyvinylidene fluoride (PVDF) membrane. This was done in a Trans-Blot® Turbo™ Transfer System (Bio-Rad). The protein-containing membrane was incubated in blocking solution (5% skim milk powder (Sigma-Aldrich®) in PBS-T) for 1h at room temperature on a rolling incubator (Labinco). After blocking, the membrane was incubated with rabbit anti-Olig2 (1:2500, Merck Millipore) and mouse anti-ß-Actin (1:2000, Abcam) diluted in blocking solution at 4°C on a rolling incubator overnight. Next day, the membrane was washed in PBS-T (5, 10 and 30min) and then incubated with horseradish peroxidase (HRP)-labelled goat anti-rabbit (1:20 000, EpiGentek) and HRP-labelled donkey anti-mouse (1:10 000, Abcam) diluted in PBS-T for 1 h at room temperature on a rolling incubator. The membrane was washed with PBS-T (5, 10, 30 min and 1h) before visualization.

Protein levels were detected using Supersignal™ West Femto Maximum Sensitivity Substrate Kit (Thermo Fisher Scientific) and visualized with ChemiDoc™ MP system (Bio-Rad). The protein detection was done using secondary antibodies labelled with an HRP enzyme. HRP catalyzes the oxidation of substrates by hydrogen peroxide, generating a recordable signal in the form of light. The chemiluminescent substrate used in this study consist of a peroxide solution and a luminol-based enhanced substrate solution. The membrane with HRP-conjugated antibodies was incubated in the chemiluminescent substrate solution resulting in a chemical reaction that emits light at 425nm which can be captured using ChemiDoc™ MP system. The analysis of the protein bands was performed through ImageLab software (Bio-Rad). Graphs were made in GraphPad Prism. All results are presented as mean ± standard deviation (SD).

3.7 Quantitative reverse transcription polymerase chain reaction analysis

Quantitative reverse transcription polymerase chain reaction (RT-qPCR) is a highly efficient method for RNA quantification. The method combines traditional RT-PCR with fluorescence. A detection of changes in fluorescence intensity during the reaction is used to follow the PCR reaction in real time (111). In this method RNA is first isolated from target tissue/cells, and further reverse-transcribed to complementary DNA (cDNA). Gene-specific PCR primers are used to

amplify a segment of the cDNA of interest. The amplified cDNA is fluorescently labelled, and the amount of fluorescence released during amplification is directly proportional to the amount of amplified cDNA. In this study a double stranded (dsDNA) binding dye was used, called SYBR Green. This dye binds to the minor groove of dsDNA and does not bind to single stranded DNA (ssDNA). During the PCR, SYBR Green binds to each new copy of dsDNA as the target sequence is amplified. The fluorescence of the bound dye is 1000-fold higher than that of the free dye, therefore this results in an increase in the fluorescence signal (112). The faster the increase of fluorescence during the PCR cycles the higher the initial amount of RNA in the sample. The cycle in which fluorescence can be detected is termed quantitation cycle (Cq), the lower the Cq values the higher initial copy number of the target (113). RT-qPCR was in this study used to validate the HCAR1 KO mice on mRNA level and to determine relative mRNA expression of Olig2 in brain tissue from P8 WT and HCAR1 KO mice (6h post HI).

3.7.1 RNA purification and cDNA construction

Brain tissue from WT and HCAR1 KO mice was pulverized in an Eppendorf tube on dry ice with a pellet pestle (Life Sciences). RNA was isolated using RNeasy Plus Micro Kit (QIAGEN), and a NanoDrop™ Spectrophotometer (Thermo Fisher Scientific) was used to measure the total RNA concentration and the RNA purity. cDNA was synthesized from 2 mg total RNA using reagents from High-Capacity cDNA Reverse Transcription Kit (Thermo Fisher Scientific) to a total of 20 µL. A 2720 Thermal Cycler (Thermo Fisher Scientific) was used to reverse transcribe RNA to cDNA. Reagents, volume per reaction in synthesis of cDNA and reaction conditions are listed in Appendix, section B.

3.7.2 RT-qPCR

The cDNA was diluted 1:10 in RNase free water, mixed with SYBR™ Green PCR Master Mix (Thermo Fischer scientific) and primers targeting genes of interest (Primer sequences are listed in table 1). A MicroAmp® Fast 96-well Reaction Plate (Thermo Fischer Scientific) was loaded with the reaction mixture, sealed with MicroAmp™ Optical Adhesive Film (Thermo Fischer Scientific) and centrifuged in a Microplate Centrifuge (VWRInternational). The RT-qPCR reaction was carried out in a StepOnePlus™ Real-Time PCR System (Thermo Fisher Scientific). RT-qPCR mixture reagents, volume per reaction and reaction conditions are listed in Appendix, section B.

Table 1. Primer sequences used for RT-qPCR

Gene	Forward/Reverse	Sequence
Olig2	Forward	TGAAGCGATGGAGAGATGCG
	Reverse	CCCAGACCCTTGGAGTGTTC
HCAR1	Forward	AGTTTCTCTCGTGGGTGCAG
	Reverse	GCCTATCCGAACACTAGGGC
GAPDH	Forward	TCGTCCCGTAGACAAAATGGT
	Reverse	CGCCCAATACGGCCAAA

Abbrevations: Olig 2= Oligodendrocyte transcription factor 2, HCAR1= Hydroxycarboxylic acid receptor 1, GAPDH= Glyceraldehyde 3-phosphate dehydrogenase.

3.7.3 Data analysis

Relative RNA levels were determined by analysing changes in SYBR green fluorescence during RT-qPCR, and the standard curve method was used. A standard curve was made for each gene (HCAR1, Olig2 and GAPDH) using serial dilutions of cDNA from the wild type mice (1:5, 1:10, 1:50, 1:100, 1:500 and 1:1000 dilutions). Two technical duplicates were measured of the samples, and the mean of the duplicates was used in the further data analysis. Expression levels of all genes were normalized to the reference gene GAPDH. Adipose tissue was used as positive control for HCAR1, and negative control for Olig2. The raw data was analysed using SDS software version 2.4.1 (Applied Biosystems), and Microsoft Excel. GraphPad Prism was used for statistical analysis and construction of graphs. Unpaired t-test was used for the statistical analysis All results are presented as mean ± SEM.

3.8 Fluorescent in situ hybridization

RNA fluorescent in situ hybridization (RNA-FISH), an mRNA detection method, combined with immunohistochemistry was used for detection and localization of HCAR1 in the mouse brain. In RNA-FISH the sample is fixed, and the endogenous RNA is hybridized with probes that are labelled with a fluorescent dye. The probes are designed to be complementary to the RNA of interest, and the hybridization of probes to the RNA molecule makes it detectable *in situ* by fluorescent microscopy (114).

3.8.1 Sample preparation

C57BL/6N wild type mice were perfused *in vivo* with 4% PFA, dissected out stored in 4% PFA for 24 h before immediately proceeding with cryopreservation. In this experiment it was important to proceed immediately to cryopreservation after 24 h fixation in 4% PFA instead of keeping the samples in 0.4% PFA as this could reverse the fixation process and activate ribonucleases leading to degradation of RNA. After cryo-sectioning it was also important to store the sections in -80°C for minimal activity of RNases.

Cryopreservation

Cryopreservation involves freezing down the sample, it was therefore important to remove the intracellular water to prevent expansion and crystallization which could cause cellular damage. Dehydration was done by immersing the brain in increasing concentrations of sucrose. As the tissue is placed in a hypertonic solution, water will move out of the cells by exosmosis (115). The sucrose saturation of the tissue was performed in three steps. First the brains were incubated in 10% sucrose (diluted in PBS) until the tissue had sunken to the bottom of the container. Then the brains were incubated in 20% sucrose (diluted in PBS), followed by 30% sucrose (diluted in PBS), each time allowing the tissue to sink to the bottom of the container. The sucrose saturation was done at 4°C. The saturated brain tissue was frozen in Epredia™ Neg-50™ Frozen Section Medium (Thermo Fisher Scientific) on dry ice and stored in an airtight container at -80°C.

Cryosectioning

A cryostat was used to cut the brain tissue into thin sections. Thin sections are needed to study the cells with high resolution in the microscope. In this experiment a CryoStar™ NX70 Cryostat (Thermo Fisher Scientific) was used. The cryopreserved sections were cut in -20 °C as this turned out to be the best temperature for fixed mouse brains. At higher temperatures the sections curled up, and at lower temperatures the sections crumbled up. The sections for this experiment were cut 18 µm thick and mounted on SuperFrost Plus™ Adhesion slides (Thermo Fisher Scientific) and stored at -80°C.

3.8.2 RNA-FISH combined with IHC

RNA-FISH combined with IHC was used for detection and localization of HCAR1 in the mouse brain. This was done following the RNAscope® Multiplex Fluorescent Reagent Kit v2 Assay user manual, and the Integrated Co-Detection Workflow technical note.

The slides were washed with PBS in a slide rack for 5 min while moving the rack up and down to remove the embedding media. Then the slides were baked in a heating incubator (Termaks) for 30 min at 60°C and post-fixed in 4% PFA in PBS for 15 min at 4°C. The tissue was dehydrated in an alcohol gradient (50% EtOH 5 min, 70% EtOH 5 min and 100% EtOH 5min x 2 at room temperature) and put on the bench to air dry for 5 min. Following the sections were incubated with RNAscope® Hydrogen peroxide (ACD Bio) for 10 min at room temperature and washed with distilled water.

For target retrieval, the slides were slowly submerged into a mildly boiling (98-102°C) RNA scope® 1X Target Retrieval Reagents solution (ACD Bio), and boiled for 15 min. After the target retrieval, the slides were washed in distilled water and PBS-T. A hydrophobic barrier was drawn around the sections using an ImmEdge™ hydrophobic barrier pen (Thermo Fisher Scientific).Then the slides were placed in a RNAscope® EZ-Batch™ Slide Holder (ACD Bio) and incubated with rabbit anti-Olig2 (1:100, Merck Millipore) diluted in Co-detection Antibody Diluent (ACD Bio). Incubation was done in a HybEZ™ Humidity Control Tray (ACD Bio) containing a humidifying paper (wet with distilled water) at 4°C overnight.

Following primary antibody incubation, the slides were washed with PBS-T, and post primary fixed in 10% Neutral Buffered Formalin (NBF)(Sigma-Aldrich) for 30 min at room temperature. Then the slides were washed in PBS-T, placed in the slide rack, and incubated with RNAscope® Protease Plus (ACD Bio). The Slide rack were placed in a pre-heated (30 min at 40°C) HybEZ™ Humidity Control Tray (ACD Bio) containing a humidifying paper (wet with distilled water) and incubated for 30 min at 40 °C in a HybEZ™ Oven (ACD Bio). After incubation the slides were washed with distilled water in a RNAscope®EZ-Batch™ Wash tray (ACD Bio).

Following the sections were incubated with RNAscope® Probe-HCAR1 (ACD Bio) for 2 hours, RNAscope® Multiplex FL v2 Amp 1 (30 min), Amp 2 (30 min), and Amp3 (15 min) (ACD Bio), Opal™ 570 (1:1500, ACD Bio) diluted in tyramide signal amplification (TSA Buffer) for 30 min and finally RNAscope® Multiplex FL v2 HRP blocker (ACD Bio) for 15 min . All incubations were done in a HybEZ™ Oven at 40°C. The slides were washed with 1X RNAscope® Wash Buffer (ACD Bio) in the wash tray (2 min x 2) between each incubation.

Then the sections were incubated with Alexa Fluor 488 goat anti-rabbit (1:400, Invitrogen) diluted in Co-Detection Antibody Diluent (ACD-Bio) for 30min at room temperature and washed with

PBS-T. Following the secondary antibody incubation, the sections were incubated with RNAscope® Multiplex FL v2 DAPI (ACD Bio) for 30 sec at room temperature and mounted with ProLong™ Glass Antifade Mountant (Thermo Fisher Scientific). Cover glass thickness was 0.13-0.17mm. The cover glass was sealed with nail polish to prevent the sections from drying out and stored in dark at 4 ºC until observation in confocal microscope. For imaging the results, a Leica TCS SP8 STED confocal microscope with Leica LASX software was used. The images were taken with a 40x oil-immersion objective (NA 1.3). All the images were analysed using the ImageJ open-source, Java based imaging program.

4. Results

4.1 mRNA expression of Olig2 and HCAR1

Quantitative reverse transcription polymerase chain reaction (RT-qPCR) was used with the goal to validate the HCAR1 KO mice, as no HCAR1 mRNA should be expressed. This method was also used to study the expression of oligodendrocytes on mRNA level. RNA was isolated from the contralateral hemisphere of P8 WT and HCAR1 KO mice. RNA isolated from adipocytes was used as positive control for the HCAR1 analysis, as it is known that HCAR1 is highly expressed in these cells (116). As oligodendrocytes are only present in the brain, adipocytes were used as negative control for the mRNA expression analysis of Olig2.

The HCAR1 expression was significantly lower in the HCAR1 KO compared with the WT mice (Figure 4.1, A, Relative expression HCAR1/GAPDH: WT contra: 1.04 ± 0.20, KO contra: 0.33 ± 0.07, p=0.03, df 4, n=3). As expected, HCAR1 had a higher expression in the adipocytes compared with the brain tissue.

The mRNA expression of Olig2 in WT and HCAR1 KO mice do not seem to differ in the contralateral side. (Figure 4.1, B, Relative expression Olig2/GAPDH: WT contra: 1.00 ± 0.04, KO contra: 0.94 ± 0.02, p=0.312, df 4, n=3) As expected, Olig2 was not expressed in the adipocytes.

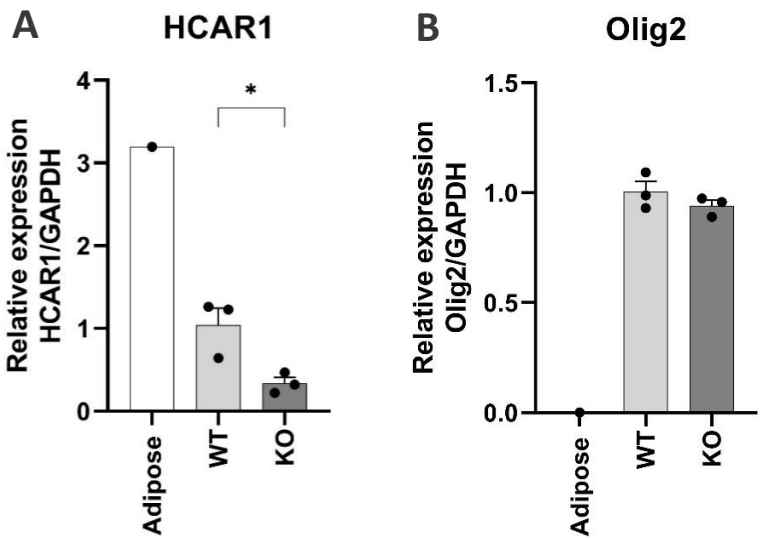

Figure 4.1: HCAR1 and Olig2 expression in WT and HCAR1 KO mice. A: HCAR1 mRNA expression, normalized to GAPDH in WT (light grey bar) and HCAR1 KO (dark grey bar) mice. Positive ctrl: adipose (white bar). **B:** Olig2 mRNA expression, normalized to GAPDH in WT (light grey bar) and HCAR1 KO (dark grey bar) mice. Neg ctrl: adipose. *p<0.05. Each point represents one sample/mouse. Error bar = SEM. WT n=3, KO n=3.

4.2 The effect of HCAR1 on oligodendrocytes and cell proliferation

Hypoxia ischemia (HI) was induced in 8 days old HCAR1 knockout and C57BL/6N wild type mice to investigate the role of HCAR1 on oligodendrocytes and proliferated cells after neonatal HI. The mice used in this study were sacrificed 7 days post HI. The number of DAPI+, Olig2+, Brdu+ and APC+ cells was assessed by immunohistochemistry on coronal mouse brain sections, and the area of interest was the peri-infarct zone surrounding the ischemic core.

In the peri-infarct zone, the total number of cells was increased by 38% in the affected ipsilateral hemisphere compared with the contralateral hemisphere in HCAR1 KO mice (Figure 4.3, C-D, Q, DAPI+ cells/0.1 mm^2: contra 12.6 ± 0.71, ipsi 17.4 ± 1.0, p=0.005, df 50, n=15 mice) A 25% increase of total cells in the ipsilateral side in WT mice was also observed, although this was not statistically significant (Figure 4.3, A-B, Q, DAPI+ cells/0.1 mm^2: contra 14.0 ± 0.9, ipsi 17.5 ± 1.2, p=0.142, df 50, n=12). As the quantification of total cells showed a trend of increased number of cells in the ipsilateral hemisphere for both the KO and WT, the further counting of cells was not normalized to DAPI, as this could give incorrect presentation of the data. Therefore, the following counting of cells is presented as number of positive cells/area (cells/0.1mm^2).

To look at the effect of HCAR1 on oligodendrocyte survival after HI, we assessed the number of mature (and nearly mature) oligodendrocytes, using the marker APC, which labels pre- and myelinating oligodendrocytes. As expected, the number of APC+ cells was reduced in the affected ipsilateral hemisphere compared with the contralateral hemisphere in WT mice, demonstrating a loss of oligodendrocytes after HI. We detected a similar reduction of APC+ cells on the ipsilateral side in HCAR1 KO mice (Figure 4.2, E-H, M, APC+ cells/0.1 mm^2: WT contra 2.42 ± 0.20, ipsi 1.65 ± 0.16, p=0.042, df 50, n=12. KO contra 2.12 ± 0.18, ipsi 1.31 ± 0.16, p=0.012, df 50, n=15), suggesting no effect of HCAR1 on oligodendrocyte survival after HI.

A consequence of cerebral hypoxia ischemia is oligodendrocyte death and damage, which in turn leads to demyelination and neurological deficits. An important goal for brain tissue repair after injury is therefore to be able to stimulate the production of new oligodendrocytes to remyelinate the axons. To study the effect of HCAR1 on oligodendrocytes, we used the general oligodendrocyte marker Olig2, which labels all oligodendrocyte lineage cells. In the peri-infarct zone, the number of oligodendrocytes was increased by 58,5% in the affected ipsilateral hemisphere compared with the contralateral hemisphere in WT mice (Figure 4.3, E-F, R, Olig2+

cells/0.1 mm^2: contra 4.1 ± 0.33, ipsi 6.5 ± 0.58, p=0.026, df 50, n=12). No statistically significant increase of oligodendrocytes in the ipsilateral hemisphere compared with the contralateral hemisphere was detected in HCAR1 KO mice (Figure 4.3, G-H, R, Olig2+ cells/0.1 mm^2: contra 4.6 ± 0.39, ipsi 5.5 ± 0.69, p=0.775, df 50, n=15).

We then assessed cell proliferation by counting the number of cells that were positive for the proliferation marker BrdU. The number of newly proliferated BrdU+ cells more than doubled in the affected ipsilateral hemisphere compared with the contralateral hemisphere in WT mice (Figure 4.3, I-J, S, BrdU+ cells/0.1 mm^2: contra 1.14 ± 0.19, ipsi 2.66 ± 0.58, p=0.0194, df 38, n=12). In KO mice, however, there were no statistically significant increase in the number of newly proliferated cells in the ipsilateral hemisphere compared with the contralateral hemisphere (Figure 4.3, K-L, S BrdU+ cells/0.1 mm^2: contra 0.96 ± 0.07, ipsi 1.5 ± 0.19, p=0.91, df 38, n=9).

From the quantification of proliferating cells, it appears that HCAR1 KO mice have impaired cell proliferation after HI. Thus, we wanted to see if this was the case for oligodendrocyte proliferation by counting cells that were both BrdU+ and Olig2+. The number of proliferated oligodendrocytes was increased in the ipsilateral hemisphere after HI in WT, but did not have a statistically significant increase in HCAR1 KO mice (Figure 4.3, M-P, T, BrdU+ Olig2+ cells/0.1 mm^2: WT contra 0.46 ± 0.08, ipsi 0.95 ± 0.16, p=0.012, df 38, n=12. KO contra 0.38 ± 0.04, ipsi 0.60 ± 0.06, p=0.75, df 38, n=9). These data indicate impaired oligodendrocyte proliferation following hypoxia ischemia in mice lacking the lactate receptor.

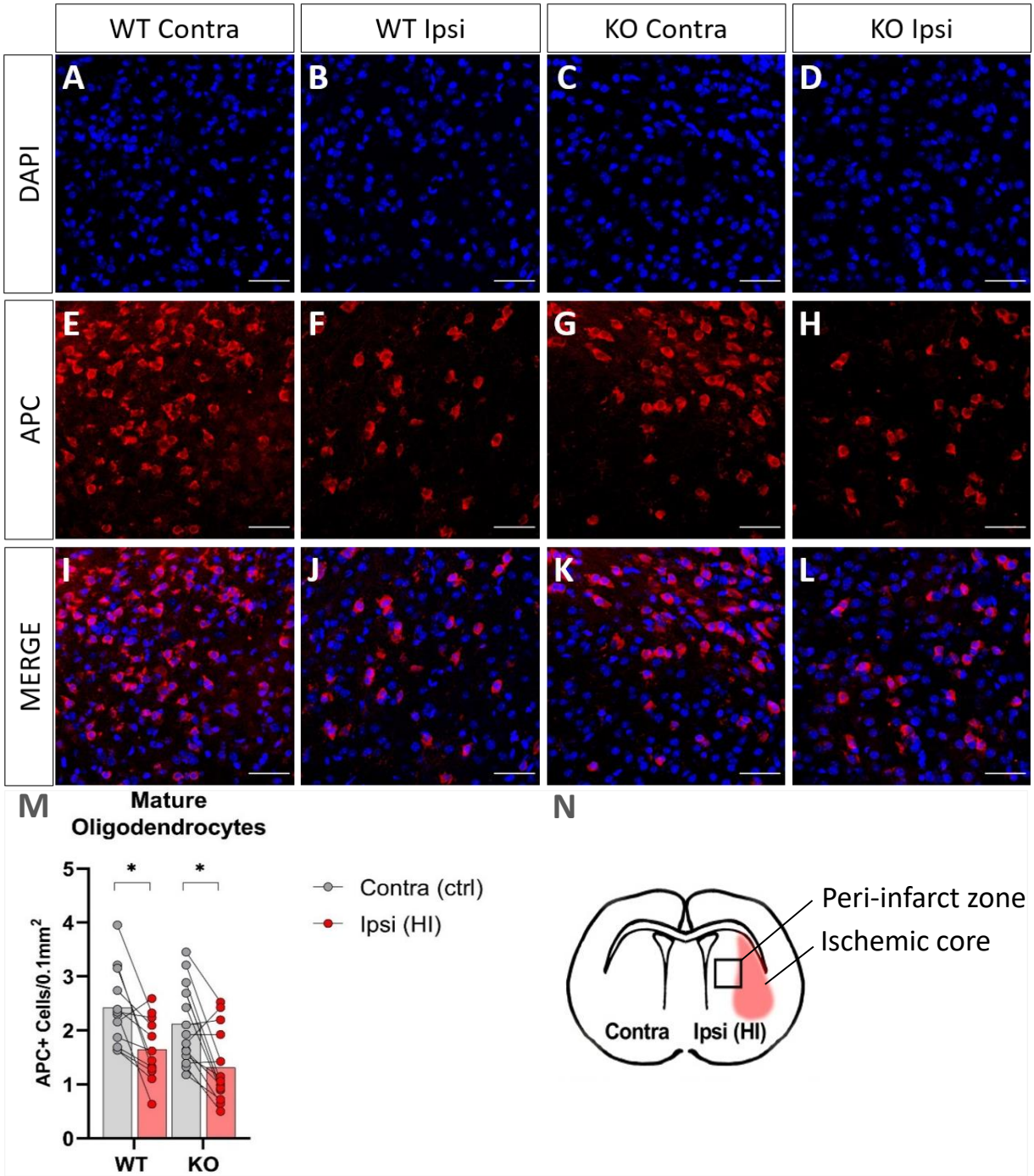

Figure 4.2: The effect of HCAR 1 on oligodendrocyte survival after HI. A-L: Confocal images from the peri-infarct zone (ipsi) and corresponding contralateral area (contra) of coronal mouse brain sections from WT (left) and HCAR1 KO (right). Sections are labelled with DAPI (all nuclei, blue, **A-D**), APC (mature and nearly mature oligodendrocytes, red **E-H**). Merged images with DAPI and APC are shown in **I-L**. Scale bar = 50µm. **M:** Density of APC+ cells in the peri-infarct zone of the ipsi- (red bars) and contralateral (grey bars) hemispheres of WT and HCAR1 KO mice. *p<0.05. Each point represents one sample/mouse. Ipsi- (red point) and contralateral hemisphere (grey point) from the same mouse are indicated with a line. WT n= 12 KO n=15. **N:** Illustration of a coronal mouse brain section indicating the peri-infarct zone were pictures were captured (black square).

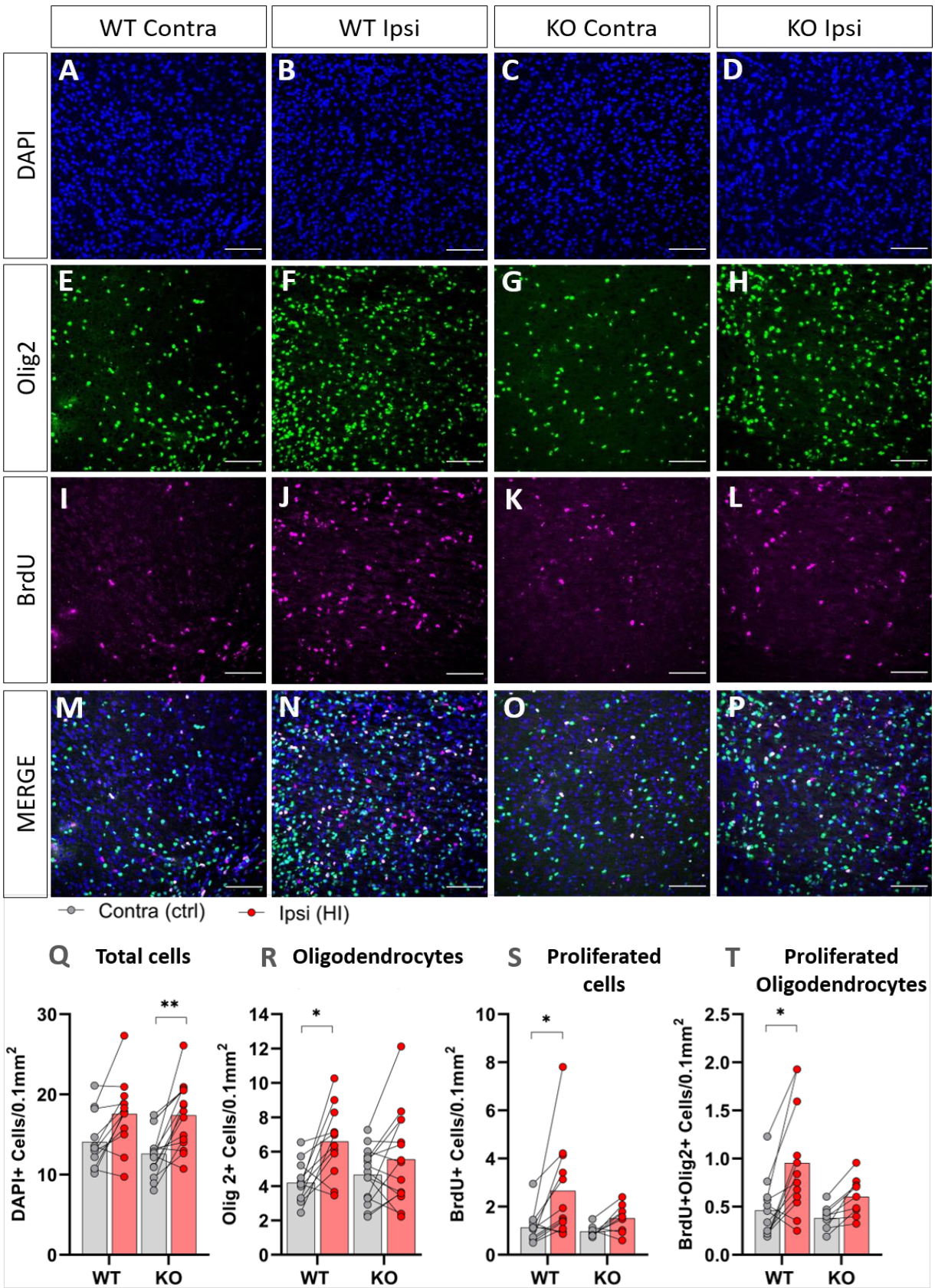
WT Contra
WT Ipsi
KO Contra
KO Ipsi
DAPI
Olig2
BrdU
MERGE
A
B
C
D
E
F
G
H
I
J
K
L
M
N
O
P
Contra (ctrl)
Ipsi (HI)
Q Total cells
R Oligodendrocytes
S Proliferated cells
T Proliferated Oligodendrocytes
DAPI+ Cells/0.1mm2
Olig 2+ Cells/0.1mm2
BrdU+ Cells/0.1mm2
BrdU+Olig2+ Cells/0.1mm2
WT
KO
**
*

Figure 4.3: The effect of HCAR1 on cell- and oligodendrocyte proliferation. A-P: Confocal images from the peri-infarct zone (ipsi) and corresponding contralateral area (contra) of coronal brain sections from WT (left) and HCAR1 KO mice (right). Sections are labelled with DAPI (all nuclei, blue, **A-D**), Olig2 (oligodendrocytes, green, **F**-**H**) and BrdU (proliferating cells, magenta **I-L**). Merged images with DAPI, Olig2 and BrdU are shown in **M**-**P**. Scale bar = 100µm. **Q**-**T**: Density of DAPI+ cells (i.e. total cells, **Q**), Olig2+ cells (oligodendrocytes, **R**), BrdU+ cells (all proliferating cells, **S**) and proliferated oligodendrocytes (i.e. cells that were both Olig2+ and BrdU+, **T**) in the peri-infarct zone of the ipsi- (red bars) and contralateral (grey bars) hemispheres of WT and HCAR1 KO mice. *$p<0.05$; **$p<0.01$. Each point represents one sample/mouse. Ipsi- (red point) and contralateral hemisphere (grey point) from the same mouse are indicated with a line. WT n= 12, KO n=9-15.

4.3 Protein analysis of oligodendrocytes in WT and HCAR1 KO mice

Further we wanted to analyse Olig2 protein levels with western blotting, to check if the data from IHC yielded the same results in a western blot analysis. Tissue from the striatum of P8 HCAR1 KO and WT mice (6h post HI) was used for the protein analysis. Protein extracts were separated by SDS-PAGE and blotted on a PVDF membrane. The membrane was immunolabelled with the oligodendrocyte marker Olig2, and ß-Actin was used as loading control. The blots are presented in figure 4.4A, showing a Olig2 positive band at approximately 32 kDa, and ß-Actin positive band at 45 kDa, which correspond to the expected size of the endogenous proteins. The western blot data show a trend of higher Olig2 protein expression in the HCAR1 KO striatum in the affected ipsilateral side as well as the contralateral side compared with the wild type (Figure 4.4, B, Olig2 expression relative to ß-Actin: WT contra 0.80 ± 0.06, n=3, ipsi 1.01 ± 0.21, n=2, KO contra 1.02 ± 0.06, ipsi 1.13 ± 0.02 n=2). Due to lack of mouse tissue, the ipsilateral and contralateral samples were obtained from different individuals and no statistical analysis was performed.

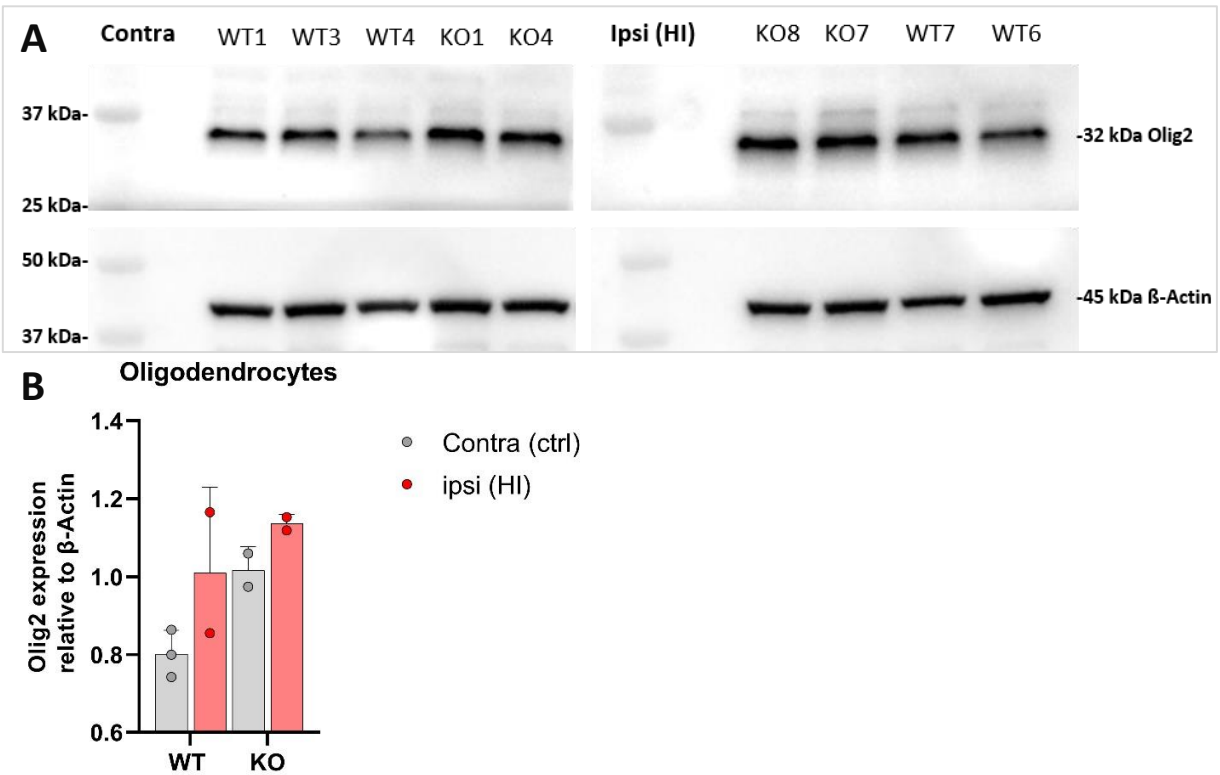

Figure 4.4: Olig2 protein expression in WT and HCAR1 KO mice. A: Western blot of striatum samples from P8 WT and HCAR1 KO mice (6h post HI). Left membrane represents the contralateral striatum and right membrane represents the ipsilateral striatum (affected side) in WT and HCAR1 KO mice. A clear band was detected, for Olig 2 (32 kDa), and for ß-Actin (45 kDa). **B:** Olig2 expression relative to ß-Actin in striatum of the ipsi- (red bars) and contralateral (grey bars) hemispheres of WT and HCAR1 KO mice. Each point represents one sample/mouse, ipsi- (red point) and contralateral (grey point). Error bars = SD, n= 2.

4.4 in situ detection of HCAR1 in the mouse brain

Although HCAR1 has been detected in pial fibroblasts in the mouse brain (117), its expression in other brain cells is disputed (82). Since antibodies for HCAR1 have been found to be unspecific (82), we performed RNA fluorescent *in situ* hybridization (RNA-FISH), an mRNA detection method, combined with immunohistochemistry for detection and localization of HCAR1 in the mouse brain. This approach revealed that HCAR1 was expressed in in Olig2+ oligodendrocytes in the corpus callosum (Figure 4.5). No signal was detected in the negative control (not shown)

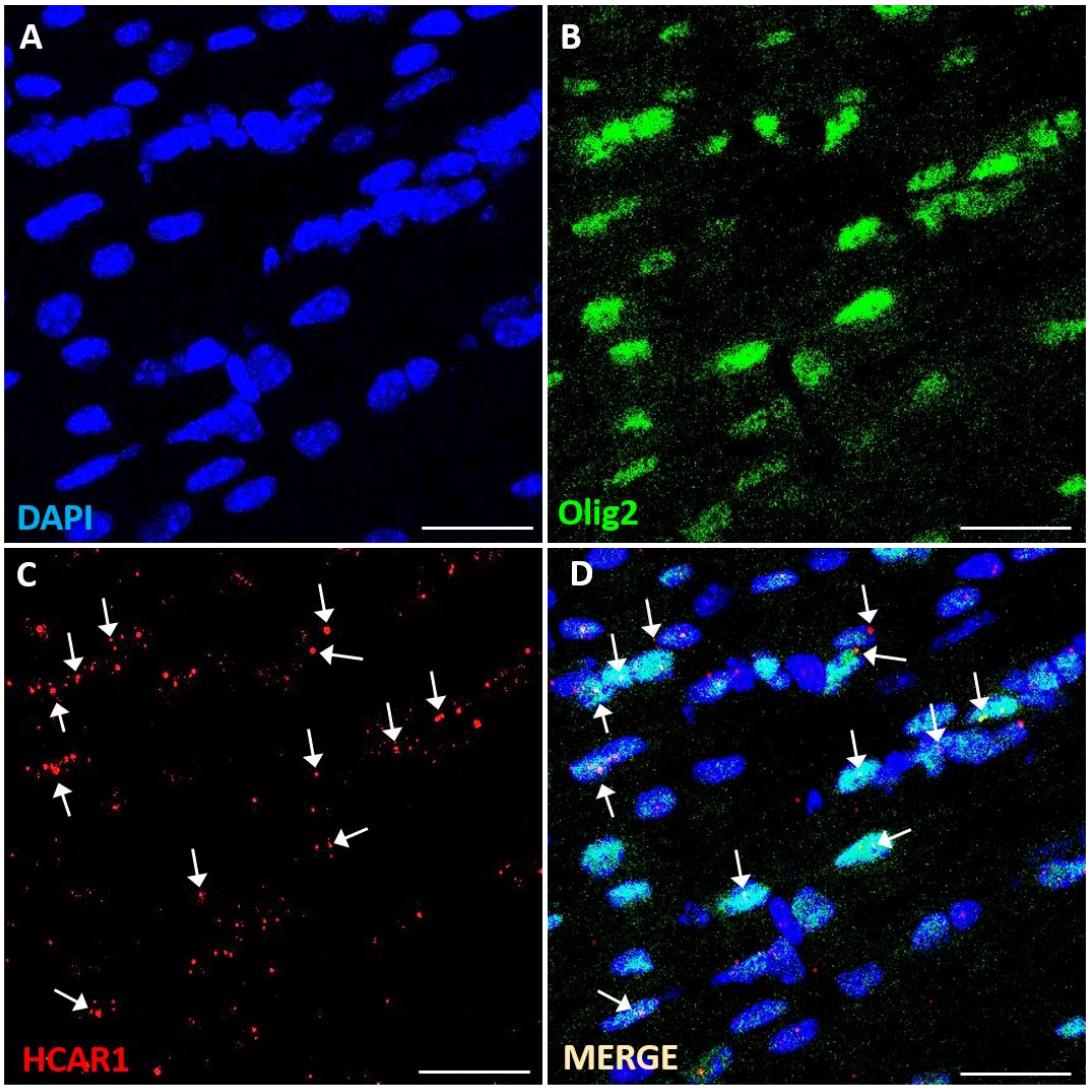

Figure 4.5: HCAR1 localization in oligodendrocytes in the corpus callosum. A-D: Confocal images from Corpus callosum in coronal brain section from WT mouse, combining fluorescent in situ hybridization for hydroxycarboxylic acid receptor 1 (HCAR1 mRNA, red **C**) with immunohistochemistry for Olig 2 (oligodendrocytes, green, **B**) and DAPI (all nuclei, blue **A**). **D:** Merged image with DAPI, Olig2 and HCAR1. white arrows: DAPI+ Olig2+ HCAR1+ cells. Scale bar = 25 µm.

HCAR1 expression was also detected in other brain areas including the subventricular zone (SVZ), neocortex and the granular cell layer of the dentate gyrus (DG) of the hippocampus (Figure 4.6), indicating that HCAR1 is expressed in a variety of other cells. Our group is currently optimizing the RNA- FISH method combined with IHC to detect HCAR1 expression in different cell types in the brain. A co-staining with the neuronal marker TUJ1 was done in this experiment, but no signal was detected (not shown).

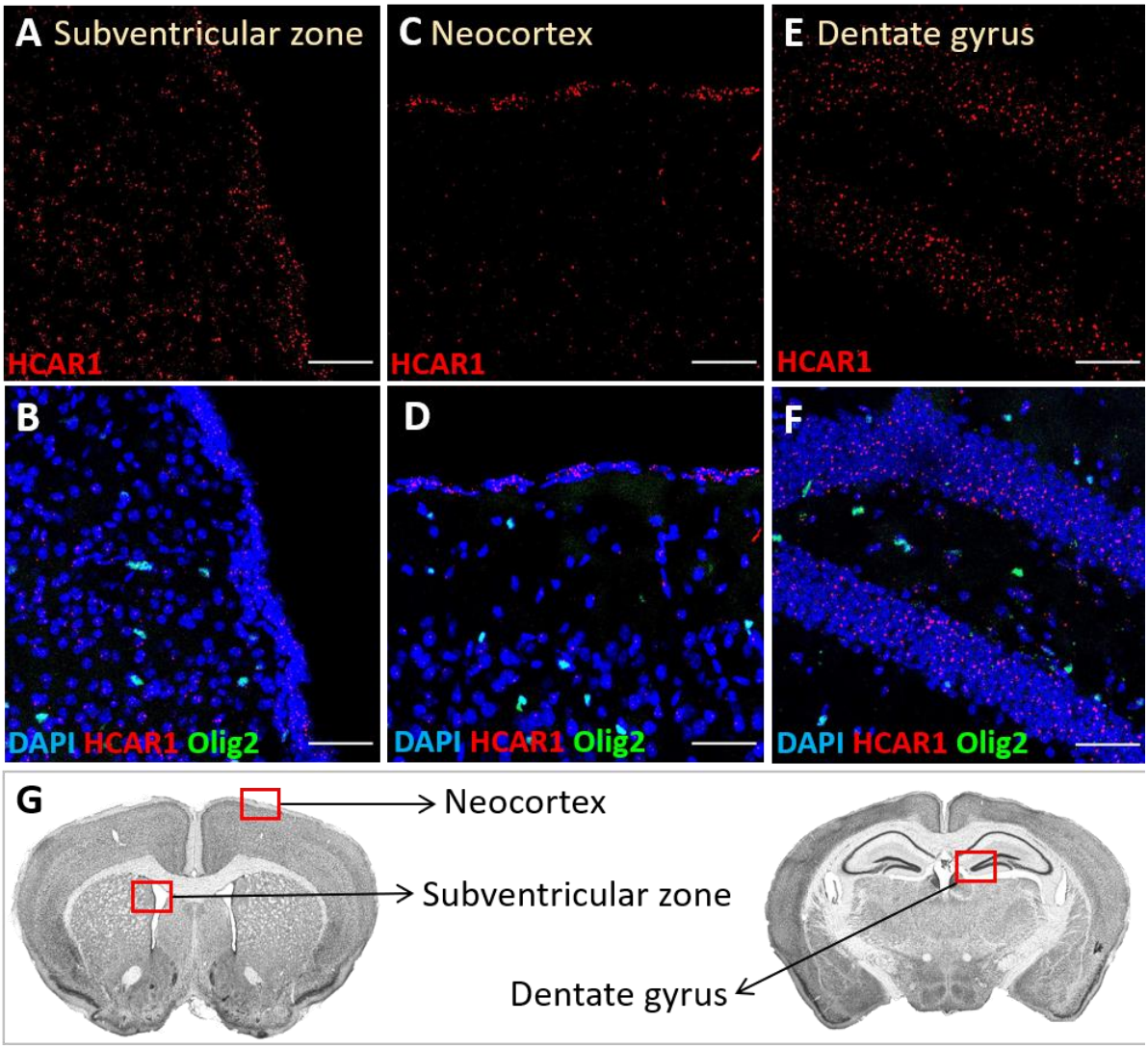

Figure 4.6: HCAR1 localization in different structures of the mouse brain. A-F: Confocal images from the Subventricular zone (**A-B**), Neocortex (**C-D**) and Dentate Gyrus of the hippocampus (**E-F**) in mouse brain sections, combining fluorescent in situ hybridization for hydroxycarboxylic acid receptor 1 (HCAR1 mRNA, red) with immunohistochemistry for Olig2 (oligodendrocytes, green) and DAPI (all nuclei, blue). Images in the top panel (**A, C, E**) show HCAR1 only, while merged images with all markers included are shown below (**B, D, F**). Scale bar = 50 µm. **G:** Coronal mouse brain sections indicating the areas where pictures were captured (red squares). Obtained from brainmap.org (118).

5. Discussion

In this section I will first discuss the use of animals in research, followed by a discussion of the methods used in this study. Then I will proceed to discuss the experimental results in comparison to the expectations and previous findings. Lastly, I will present suggestions for further work.

5.1 Discussion of methods

5.1.1 The use of mouse models in research

It is important to do an evaluation whether it is possible to use a non-animal model before animal models are applied, as *in vitro* models are a much more ethical alternative. When studying the role of HCAR1 after hypoxia ischemia, *in vitro* models are insufficient to adequately resemble the highly heterogenous condition of hypoxia ischemia. Therefore, the use of an animal model was considered necessary for further investigations of the lactate receptor.

It may seem paradoxical to use an animal model when studying the one organ that most clearly distinguishes humans as complex and advanced organisms from other animals. However, many of the basic structures and functions are conserved across all mammals. Complex thoughts and functions of the human brain are built on a foundation of simpler mental processes found in animals, thus animal models can be used to gain insight into the complex human brain and nervous system (119).

A mouse model is used for this study. Mice have for a long time served as models of human biology and disease for a number of reasons (120). Firstly, the high genetic similarity to humans (over 90%), gives a great advantage. (121). It is also relatively easy to manipulate their genome, making it possible to create knock-out mice, which can be used to study selected genes. They breed quickly, have multiple offspring at once, and one can easily interbreed them to achieve genetically identical strains. In addition, mice are considered ethically less difficult to use than other phylogenetic human relatives, such as primates.

Although there are striking genetic homologies between mice and humans, mice often respond to experimental interventions in ways that differ from humans. When using mice in medical research to predict human outcomes one need to take account of the evolved differences as well as the similarities between the two species (122).

In this study, wild type mice of the strain C57BL/6N and HCAR1 knock-out mice were used. Genotypes were determined by polymerase chain reaction (PCR) analysis of DNA samples extracted from mouse ears (83), and only homozygote mice were used. Instead of solely knocking out the HCAR1 gene, the exon was replaced by a gene cassette encoding β-galactosidase (LacZ) and neomycin resistance, which reduces the possibility of false negative genotyping results. Mice at postnatal day 8 were used for this study. At P8, the mouse brain is histologically similar to a newborn infant, cerebral cortical neuronal layering is complete, the germinal matrix is involuting, and white matter has undergone little myelination (123).

A problem that arose in this study regarding the use of KO mice was that they were more difficult to breed compared with the WT mice. The KO mice had fewer offspring, and there were cases where the mother ate up their babies. This affected the number of KO animals used in this study. When using knock-out mice it is also important to notice that other KO mice have shown to develop compensatory mechanisms by other genes, thus hiding the effect of the missing one (124, 125). This is not considered as a critical factor, but something to be aware of as compensation by other genes could potentially impair the reliability of the results.

5.1.2 Mouse model for cerebral HI

As previously described, hypoxia ischemia is a result of multiple heterogenous conditions where many factors play a role. The duration of ischemia, adequate blood pressure, localization and severity of the injury, as well as age, genes, and sex all together play a role for the outcome of the condition. With so many variables it is hard to find an ideal model that mimics the clinical human condition. However, common for all pathologies that involve cerebral HI are that they result in impaired cerebral blood flow and oxygen delivery to the brain. The widely used Levine method (126), modified for use in neonatal mice (127) was in this study used to induce hypoxia ischemia in WT and HCAR1 KO mice. Using an animal model for HI allows for a controlled environment with controlled variables as well as reproducible injury in the animals. This is hard in the human situation that has lots of uncontrollable variables and thereby make clinical studies complicated.

A well-known problem with the Levine method is its variation in lesion size, and the mortality under and after the surgery. Despite this, the method provides a well-defined localization of the ischemic lesion, high reproducibility, and short surgery time as well as anaesthesia time (126). In

addition this method causes injury to one side of the brain remarkably similar to that found in human babies (128), and was therefore considered the best model for HI in this study.

The advantage of using *in vivo* models is the presence of intact cerebral vasculature which is essential to study the pathophysiology of HI. *In vitro* models alone, such as tissue culture, brain slices and organoids cannot thoroughly evaluate HI and its consequences given the importance of brain vasculature to study the effect of abnormal brain perfusion (129). Thus, animal models are required to reproduce specific aspects of the human condition in order to understand the complex pathophysiology of cerebral HI, and to find preventive and therapeutic approaches (130, 131).

5.1.3 Primer specificity and RNA purity

An important factor for the RT-qPCR is the specificity of the primers. The primers used should only be specific to the gene of interest. Non-specific primers could result in amplification of other similar genes. In this study RT-qPCR was used with the goal to validate the HCAR1 KO mice on mRNA level. All the HCAR1 KO mice used in this study were validated on genome level, and thus no mRNA should be detected. In the RNA analysis however, HCAR1 RNA was detected in the KO mice, indicating non-specificity of the primers used in this study. As HCAR1 and HCAR2 exhibits substantial homology (77), the detected mRNA in the KO may be HCAR2. Another important factor is the RNA purity, which was checked on the isolated RNA from WT and HCAR1 mice using a NanoDrop™ Spectrophotometer. Purity of RNA can be evaluated by determining the ratio of absorbance readings at 260 nm and 280 nm (A260/A280). This ratio offers an estimate of RNA purity (absorbing at 260 nm) with respect to contaminants such as proteins (absorbing at 280 nm). Pure RNA has an A260/A280 ratio of 1.8-2.1 (132). All the samples in this study gave a ratio between 1.9 and 2.1, indicating pure RNA.

5.1.4 The use of immunostaining and immunoblotting to quantify number of cells and amount of proteins

Immunohistochemistry was the main method used for the quantification of different cell types in this study. Prior to IHC the tissue was fixed with by paraformaldehyde, a cross-linking fixative. A consequence of using a cross-linking fixative, is that the epitopes can be cross-linked and covered making them unavailable for antibody binding. To solve this problem an antigen retrieval step was carried out prior to immunolabelling. A heat-induced antigen retrieval was used to enhance tissue antigenicity and reproducibility of the staining. The protein cross-linkages that occur with aldehyde fixation is broken down by the heat, thus enhancing the antigenicity (133). Even though

IHC uses specific antibodies, non-specific binding of the antibodies could occur. Before immunolabelling, the tissue was therefore incubated with a blocking solution which covers up unwanted binding sites. In addition, we used well known and widely used antibodies in this study. The staining was verified in the microscope as the different antibodies label specific components of the cell. The staining was also verified by making sure that our microscopic findings matched the description from the literature. The primary antibody Olig2, was also used in a western blot analysis. The specificity of the antibody was thereby confirmed by detection of a Olig2 positive band corresponding to the size of the endogenous protein.

The number of cells can vary depending on the area in the brain we are studying. It was therefore important in the IHC experiment to be consistent when choosing the area we imaged, i.e. the area of the brain we quantified the different cell types. All the images in this study were captured in the peri-infarct zone surrounding the ischemic core, and in the corresponding area of the contralateral side. A problem concerning the use of IHC to quantify cells is that one does not sample the entire brain. To cover enough areas of the brain we used several section pr mouse and captured several images pr section. Alternatively, one could isolate the area of interest, and quantify the cells using fluorescence-activated cell sorting (FACS). This method would include more cells, but the advantage with IHC is the use of tissue sections that allows for more accurate localization of the cells in the brain. Another problem concerning the use of IHC to quantify cells is that the quantification could be biased. To avoid this problem the imaging and image analysis were blinded to prevent us from having knowledge of which genotype that were analysed, thus limiting unintentional or subjective observation biases that may skew data interpretation.

Western blotting is another method that works by exploiting the principal of how antibodies specifically bind to the antigens in the tissue. The western blot technique does not necessarily provide information of the number of cells or their localization in the brain as IHC, but rather generate a signal that is proportional to the amount of protein that exists in the sample. As western blot also provides quantitative information, it can serve as a method for validation of the IHC data. Unfortunately, we had limited access to mouse tissue and the WB analysis was therefore performed on mice with a different recovery period post HI, and only on striatum samples were analysed.

5.1.5 Probe specificity

Our group is currently implementing the RNA-FISH method combined with IHC with the goal to find out which cell types express the hydroxycarboxylic acid receptor 1. As there are no good antibodies for HCAR1 (82), RNA-FISH was considered a good method for the localization of the receptor in the mouse brain. For RNA-FISH it was important to ensure that our probe was specific to HCAR1 RNA. Using a non-specific probe could result in false positive signals, as the probe could hybridize to unwanted RNAs. To ensure probe specificity we checked the probe in the UCSC Genome Browser and chose the probe with the lowest alignment to other genes.

For RNA-FISH it was important to proceed immediately to cryopreservation after 24 h fixation in 4% PFA instead of keeping the samples in 0.4% PFA as this could reverse the fixation process and activate ribonucleases leading to degradation of RNA. As fresh tissue was a critical factor, this approach was only performed on the WT mice, as we did not have any HCAR 1 KO mice available at that time due to delay in the breeding.

5.2 Discussion of study results

Oligodendrocytes and their myelin are highly vulnerable to cerebral hypoxia ischemia as well as other forms of brain injury. After only short period of HI oligodendrocytes are acutely damaged, leading to demyelination of the axons (25). The myelin sheaths surrounding the nerve fibers are crucial for effective action potential and neuronal health, thus it is important for the brain to stimulate the production of new oligodendrocytes to remyelinate the axons after brain injury. Our group and others have previously shown that lactate can support myelination in the brain (36, 37), however, it is unclear whether this is a pure metabolic effect of lactate or dependent on the lactate receptor HCAR1. Therefore, we wanted to investigate whether the lactate receptor is involved in oligodendrocyte proliferation and survival after neonatal hypoxia ischemia.

Impaired cell proliferation in HCAR1 KO mice after HI

The generation of new cells is essential for the brain tissue repair process following a neonatal brain injury such as hypoxia ischemia. New cells are generated by increased cell proliferation and differentiation as well as upregulation of cell cycle pathway genes (134, 135). The results from this study showed that the number of newly proliferated cells more than doubled after hypoxia ischemia in WT mice. In HCAR1 KO mice however, there was no statistically significant increase in the number of proliferated cells after HI, indicating impaired cell proliferation following hypoxia ischemia in mice lacking the lactate receptor. This corresponds to previous findings in our

group, showing that HCAR1 KO mice were unable to increase cell proliferation after HI (84). In the same study a neurosphere assay performed on spheres derived from forebrains of HCAR1 KO and WT mice also showed that neurospheres lacking HCAR1 had reduced proliferation ability. A transcriptome analysis comparing WT and HCAR1 KO mice also revealed a strong upregulation of cell cycle genes in WT mice after hypoxia ischemia, but not in the HCAR1 KO mice (84). Based on this it seems that HCAR1 could have a role on cell proliferation acting as a transcriptional regulator of cell cycle genes (84). In line with this, a newly published article showed HCAR1-dependent neurogenesis after physical exercise (136), and studies form different cell lines such as breast cancer cells and osteoblasts also suggest that HCAR1 may regulate cell proliferation and differentiation (85, 137).

Impaired oligodendrocyte proliferation in HCAR1 KO mice after HI

With this knowledge we wanted to investigate the role of HCAR1 on oligodendrocyte proliferation. The immunolabelling showed that the number of oligodendrocytes in the peri-infarct zone was increased with more than 50% after HI in WT mice, whereas no statistically significant increase was detected in HCAR1 KO mice. In addition, an increase in newly proliferated oligodendrocytes was detected in the peri-infarct zone after HI in WT, but not in HCAR1 KO mice. Our group previously showed that HCAR1 KO mice had reduced induction of cell cycle response, which might explain the lack of neurogenesis and microglia proliferation in the mice lacking the lactate receptor (84). The data from this study suggest that this is not specific for only neurons and microglia, but also oligodendrocytes. In addition, our group showed that HCAR1 KO mice had a substantial deficit in the restoration of brain tissue after HI (84). The data from this study, suggesting impaired oligodendrocyte proliferation, together with previous findings showing lack of neurogenesis and microglia activation and proliferation in HCAR1 KO mice (84), may explain the reduced brain tissue repair in the mice lacking the lactate receptor. This indicates that HCAR1 could play a crucial role in the process that leads to tissue repair.

A trend of increased cell proliferation and oligodendrocyte proliferation was detected in the HCAR1 KO mice after HI, although this was not statistically significant. In this study, we had fewer HCAR1 KO mice injected with the proliferation marker BrdU, and thus fewer KO mice tested compared with the WT mice. Increasing the number of HCAR1 KO mice could possibly show a significant increase in proliferated cells and proliferated oligodendrocytes after HI.

However, there seem to be a higher increase of these cells in the WT after HI compared with the HCAR1 KO mice.

No effect of HCAR1 on oligodendrocyte survival

Further we wanted to investigate the effect of HCAR1 on oligodendrocyte survival after HI. As expected, the number of mature (and nearly mature) oligodendrocytes was reduced after injury in WT mice, demonstrating a loss of oligodendrocytes after HI. A similar reduction of mature (and nearly mature) oligodendrocytes was detected in HCAR1 KO mice, suggesting no effect of HCAR1 on oligodendrocyte survival after HI.

Remyelination involves generation of new mature oligodendrocytes, and since HCAR1 seems to play a role in oligodendrocyte proliferation, it is possible that more mature oligodendrocytes could be observed in the WT compared with the HCAR1 KO after a longer recovery period post HI. Thus, the role of HCAR1 needs to be further investigated by studying different recovery periods after HI. Since no markers for cell death was included in this study, we cannot say for sure that we are looking at cell survival, therefore, new studies should be done including the marker caspase and TUNEL assay for the detection of cell death.

Following an ischemic event the lactate levels in the brain rises (138, 139), but no additional lactate was injected in the mice in this study. Thus, the observed effect from these experiments must be due to endogenous lactate or possible baseline receptor activity.

HCAR1 is less important in the healthy brain

When investigating the total number of cells, oligodendrocytes, and proliferating cells in the contralateral hemisphere in the IHC experiments, no differences were detected between the WT and HCAR1 KO mice. Nor was it observed any differences between the two genotypes in the mRNA analysis of Olig2 in the contralateral hemisphere. Indicating that HCAR1 may be less important under normal conditions in the healthy brain.

In the protein analysis however, there seemed to be a higher Olig2 protein expression in the HCAR1 KO mice both under normal conditions and after injury compared with the wild type. The protein analysis does not necessarily say anything about the number of cells, but rather generate a signal that is proportional to the amount of protein that exist in the sample. There is a theoretical possibility that the HCAR1 KO mice have higher Olig2 expression per cell, which might explain the observed differences. In, addition, the protein analysis was performed on a low number of

individuals due to lack of mouse tissue and consequently the results from these groups are tainted with uncertainty. The protein analysis was also performed on striatum samples from mice with a 6 h recovery period, whereas the immunolabelling was performed on mice with a 7 days recovery period, with cells detected in the peri-infarct zone. Thus, a new protein analysis should be performed using mice with the same recovery period as in the IHC experiment and increase the number of animals.

HCAR1 is expressed in oligodendrocytes in the corpus callosum

Previous studies have suggested a wide distribution of HCAR1 mRNA in the brain, including in the principal neurons in the cerebral cortex, hippocampus, and cerebellum as well as in astrocytes and at capillaries (70). However, these studies used antibodies that have since been shown to be unspecific as they give similar labelling pattern in HCAR1 KO mice (82). By RNA-FISH in combination with immunohistochemistry, this study revealed *in situ* HCAR1 expression in oligodendrocytes in the corpus callosum. HCAR1 was also detected in the subventricular zone, neocortex, and the granular cell layer of the dentate gyrus of the hippocampus, indicating that HCAR1 is expressed in a variety of other cells. The labelling pattern of HCAR1 in this study matches the pattern detected in previous studies using transgenic mice that express monomeric red fluorescent protein (mRFP) under the HCAR1 promoter (117, 140). This indicates that the HCAR1 labelling is correct. In addition, the method used in this this study could be more sensitive compared with the RFP-mice as the gene expression could be detected in different cell types such as oligodendrocytes. However, the specificity of our HCAR1 FISH-probes needs to be confirmed by labelling sections from HCAR1 KO mice. This was not included in this thesis due to time considerations and a delay in the breeding of HCAR1 KO mice.

All the HCAR1 KO mice used in this study were validated on genome level using PCR (see appendix, section B). On mRNA level however, the KO mice seem to express HCAR1, although the expression was significantly lower compared with the WT mice. HCAR1 share significant sequence homology with HCAR2 (77), thus the detected mRNA in the HCAR1 KO may be HCAR2 due to nonspecific primers. For validation on mRNA level, a new mRNA analysis must be done using specific primers for HCAR1. This was not included in this thesis due to time considerations.

6. Conclusion and future perspectives

The main aim of this thesis was to investigate whether the lactate receptor is involved in oligodendrocyte survival and proliferation after neonatal cerebral hypoxia ischemia. We also wanted to find out which cell types express HCAR1 in the mouse brain.

This study revealed that HCAR1 KO mice had impaired cell- and oligodendrocyte proliferation, indicating that the lactate receptor is important for cell- and oligodendrocyte proliferation after cerebral HI. When investigating oligodendrocyte survival however, a similar reduction of oligodendrocytes was detected in both genotypes after injury, suggesting no effect of HCAR1 on oligodendrocyte survival after HI. The effect of HCAR1 on oligodendrocyte survival needs to be further investigated. For testing the effect of HI on oligodendrocytes in the two genotypes, a staining with oligodendrocyte markers combined with an apoptosis marker should be performed to determine the viability of oligodendrocytes after injury.

This study also revealed *in situ* HCAR1 expression in oligodendrocytes in the corpus callosum. HCAR1 was also detected in the subventricular zone, neocortex, and the granular cell layer of the dentate gyrus of the hippocampus, indicating that HCAR1 is expressed in a variety of other cells. This needs to be further investigated, firstly the specificity of the HCAR1 FISH-probes needs to be confirmed by labelling sections from HCAR1 KO mice. In addition, co-staining with different cell markers is needed to confirm which cell types express the lactate receptor.

Overall, this study shows that HCAR1 is important for oligodendrocyte proliferation after cerebral hypoxia ischemia. Together with previous findings showing that HCAR1 is key transcriptional regulator of brain tissue response to an ischemic insult (84), these data could in the long term contribute to treat infants after HI in which many oligodendrocytes are lost. Activating HCAR1 by elevating lactate levels during and after HI could potentially contribute to oligodendrocyte proliferation, as well as proliferation of other cell types for tissue repair. However, further investigations of the exact mechanisms in which HCAR1 works on these processes are needed. In addition, future studies using alternative animal models which more resembles humans, such as pigs, could be a promising approach for translating preclinical finding to the clinic. In the long term this could lead to a potential future treatment for neonatal cerebral hypoxia ischemia and possibly other forms of brain injury.

7. References

1. Verkhratsky A, Nedergaard M. Physiology of Astroglia. Physiol Rev. 2018;98(1):239-389.
2. Brodal P. Sentralnervesystemet Universitetsforlaget; 2013 p:29-41.
3. Marieb EN, Hoehn KN. Human Anatomy & Physiology 7th Edition Pearson 2007.
4. van Leeuwenhoek A. Epistola XXXII. Epistolae Physiologicae Super Compluribus Naturae Arcanis. 1719:309-17.
5. Virchow R. Die Cellularpathologie in ihrer Begründung auf physiologische und pathologische Gewebelehre: Good Press; 2020.
6. Maturana HR. The fine anatomy of the optic nerve of anurans--an electron microscope study. J Biophys Biochem Cytol. 1960;7(1):107-20.
7. Peters A. The formation and structure of myelin sheaths in the central nervous system. J Biophys Biochem Cytol. 1960;8(2):431-46.
8. Bunge MB, Bunge RP, Pappas GD. Electron microscopic demonstration of connections between glia and myelin sheaths in the developing mammalian central nervous system. J Cell Biol. 1962;12:448-53.
9. Rosenbluth J. A brief history of myelinated nerve fibers: one hundred and fifty years of controversy. J Neurocytol. 1999;28(4-5):251-62.
10. Spiegel I, Peles E. Cellular junctions of myelinated nerves (Review). Molecular Membrane Biology. 2002;19(2):95-101.
11. Hartline DK, Colman DR. Rapid Conduction and the Evolution of Giant Axons and Myelinated Fibers. Current Biology. 2007;17(1):R29-R35.
12. Rinholm JE, Vervaeke K, Tadross MR, Tkachuk AN, Kopek BG, Brown TA, et al. Movement and structure of mitochondria in oligodendrocytes and their myelin sheaths. Glia. 2016;64(5):810-25.
13. Gonzalez-Perez O, Alvarez-Buylla A. Oligodendrogenesis in the subventricular zone and the role of epidermal growth factor. Brain Research Reviews. 2011;67(1):147-56.
14. Elbaz B, Popko B. Molecular Control of Oligodendrocyte Development. Trends in Neurosciences. 2019;42(4):263-77.
15. Armada-Moreira A, Ribeiro FF, Sebastião AM, Xapelli S. Neuroinflammatory modulators of oligodendrogenesis. Neuroimmunology and Neuroinflammation. 2015;2:263-73.
16. Tiane A, Schepers M, Rombaut B, Hupperts R, Prickaerts J, Hellings N, et al. From OPC to Oligodendrocyte: An Epigenetic Journey. Cells. 2019;8(10):1236.
17. Sock E, Wegner M. Transcriptional control of myelination and remyelination. Glia. 2019;67(11):2153-65.
18. Bhat RV, Axt KJ, Fosnaugh JS, Smith KJ, Johnson KA, Hill DE, et al. Expression of the APC tumor suppressor protein in oligodendroglia. Glia. 1996;17(2):169-74.
19. Kurinczuk JJ, White-Koning M, Badawi N. Epidemiology of neonatal encephalopathy and hypoxic–ischaemic encephalopathy. Early Human Development. 2010;86(6):329-38.
20. Shankaran S, Pappas A, McDonald SA, Vohr BR, Hintz SR, Yolton K, et al. Childhood Outcomes after Hypothermia for Neonatal Encephalopathy. New England Journal of Medicine. 2012;366(22):2085-92.
21. Roumes H, Dumont U, Sanchez S, Mazuel L, Blanc J, Raffard G, et al. Neuroprotective role of lactate in rat neonatal hypoxia-ischemia. J Cereb Blood Flow Metab. 2021;41(2):342-58.
22. Shah PS. Hypothermia: a systematic review and meta-analysis of clinical trials. Seminars in Fetal and Neonatal Medicine. 2010;15(5):238-46.

23. Douglas-Escobar M, Weiss MD. Hypoxic-ischemic encephalopathy: a review for the clinician. JAMA Pediatr. 2015;169(4):397-403.
24. Javidi E, Magnus T. Autoimmunity After Ischemic Stroke and Brain Injury. Front Immunol. 2019;10:686-.
25. Pantoni L, Garcia JH, Gutierrez JA. Cerebral white matter is highly vulnerable to ischemia. Stroke. 1996;27(9):1641-6; discussion 7.
26. Kaneko N, Kako E, Sawamoto K. Enhancement of ventricular-subventricular zone-derived neurogenesis and oligodendrogenesis by erythropoietin and its derivatives. Front Cell Neurosci. 2013;7:235.
27. Zhao C, Fancy SP, Kotter MR, Li WW, Franklin RJ. Mechanisms of CNS remyelination--the key to therapeutic advances. J Neurol Sci. 2005;233(1-2):87-91.
28. Kornek B, Storch MK, Weissert R, Wallstroem E, Stefferl A, Olsson T, et al. Multiple Sclerosis and Chronic Autoimmune Encephalomyelitis: A Comparative Quantitative Study of Axonal Injury in Active, Inactive, and Remyelinated Lesions. The American Journal of Pathology. 2000;157(1):267-76.
29. Roth AD, Ramírez G, Alarcón R, Von Bernhardi R. Oligodendrocytes damage in Alzheimer's disease: beta amyloid toxicity and inflammation. Biol Res. 2005;38(4):381-7.
30. Sjöbeck M, Haglund M, Englund E. Decreasing myelin density reflected increasing white matter pathology in Alzheimer's disease--a neuropathological study. Int J Geriatr Psychiatry. 2005;20(10):919-26.
31. Bartzokis G, Lu PH, Tishler TA, Fong SM, Oluwadara B, Finn JP, et al. Myelin breakdown and iron changes in Huntington's disease: pathogenesis and treatment implications. Neurochem Res. 2007;32(10):1655-64.
32. McTigue DM, Tripathi RB. The life, death, and replacement of oligodendrocytes in the adult CNS. J Neurochem. 2008;107(1):1-19.
33. Fünfschilling U, Supplie LM, Mahad D, Boretius S, Saab AS, Edgar J, et al. Glycolytic oligodendrocytes maintain myelin and long-term axonal integrity. Nature. 2012;485(7399):517-21.
34. Lee Y, Morrison BM, Li Y, Lengacher S, Farah MH, Hoffman PN, et al. Oligodendroglia metabolically support axons and contribute to neurodegeneration. Nature. 2012;487(7408):443-8.
35. Morrison BM, Lee Y, Rothstein JD. Oligodendroglia: metabolic supporters of axons. Trends Cell Biol. 2013;23(12):644-51.
36. Sánchez-Abarca LI, Tabernero A, Medina JM. Oligodendrocytes use lactate as a source of energy and as a precursor of lipids. GLIA. 2001;36(3):321-9.
37. Rinholm JE, Hamilton NB, Kessaris N, Richardson WD, Bergersen LH, Attwell D. Regulation of oligodendrocyte development and myelination by glucose and lactate. Journal of Neuroscience. 2011;31(2):538-48.
38. Scheele CW. The Collected Papers of Carl Wilhelm Scheele: Kraus Reprint; 1931.
39. Ewaschuk JB, Naylor JM, Zello GA. D-Lactate in Human and Ruminant Metabolism. The Journal of Nutrition. 2005;135(7):1619-25.
40. Philp A, Macdonald AL, Watt PW. Lactate--a signal coordinating cell and systemic function. J Exp Biol. 2005;208(Pt 24):4561-75.
41. Pellerin L, Magistretti PJ. Glutamate uptake into astrocytes stimulates aerobic glycolysis: a mechanism coupling neuronal activity to glucose utilization. Proc Natl Acad Sci U S A. 1994;91(22):10625-9.

42. Pellerin L, Pellegri G, Bittar PG, Charnay Y, Bouras C, Martin JL, et al. Evidence supporting the existence of an activity-dependent astrocyte-neuron lactate shuttle. Dev Neurosci. 1998;20(4-5):291-9.
43. Schurr A, West CA, Rigor BM. Lactate-supported synaptic function in the rat hippocampal slice preparation. Science. 1988;240(4857):1326-8.
44. Hubbard JL. The effect of exercise on lactate metabolism. J Physiol. 1973;231(1):1-18.
45. Brooks GA. The Science and Translation of Lactate Shuttle Theory. Cell Metabolism. 2018;27(4):757-85.
46. Connor H, Woods HF, Ledingham JGG. Comparison of the Kinetics and Utilisation of D(–)- and L(+)-Sodium Lactate in Normal Man. Annals of Nutrition and Metabolism. 1983;27(6):481-7.
47. Sokoloff L. The brain as a chemical machine. Progress in Brain Research1992. p. 19-33.
48. Schurr A, Payne RS, Miller JJ, Rigor BM. Brain lactate, not glucose, fuels the recovery of synaptic function from hypoxia upon reoxygenation: An in vitro study. Brain Research. 1997;744(1):105-11.
49. Mergenthaler P, Lindauer U, Dienel GA, Meisel A. Sugar for the brain: the role of glucose in physiological and pathological brain function. Trends in neurosciences. 2013;36(10):587-97.
50. Garcia CK, Li X, Luna J, Francke U. cDNA Cloning of the Human Monocarboxylate Transporter 1 and Chromosomal Localization of the SLC16A1 Locus to 1p13.2-p12. Genomics. 1994;23(2):500-3.
51. Garcia CK, Brown MS, Pathak RK, Goldstein JL. cDNA Cloning of MCT2, a Second Monocarboxylate Transporter Expressed in Different Cells than MCT1 (∗). J Biol Chem. 1995;270(4):1843-9.
52. Yoon H, Fanelli A, Grollman EF, Philp NJ. Identification of a unique monocarboxylate transporter (MCT3) in retinal pigment epithelium. Biochemical and Biophysical Research Communications. 1997;234(1):90-4.
53. Wilson MC, Jackson VN, Heddle C, Price NT, Pilegaard H, Juel C, et al. Lactic acid efflux from white skeletal muscle is catalyzed by the monocarboxylate transporter isoform MCT3. J Biol Chem. 1998;273(26):15920-6.
54. Halestrap AP, Price NT. The proton-linked monocarboxylate transporter (MCT) family: Structure, function and regulation. Biochemical Journal. 1999;343(2):281-99.
55. Manning Fox JE, Meredith D, Halestrap AP. Characterisation of human monocarboxylate transporter 4 substantiates its role in lactic acid efflux from skeletal muscle. Journal of Physiology. 2000;529(2):285-93.
56. Bergersen L, Wæhaug O, Helm J, Thomas M, Laake P, Davies AJ, et al. A novel postsynaptic density protein: The monocarboxylate transporter MCT2 is co-localized with δ-glutamate receptors in postsynaptic densities of parallel fiber-Purkinje cell synapses. Exp Brain Res. 2001;137(1):523-34.
57. Rafiki A, Boulland JL, Halestrap AP, Ottersen OP, Bergersen L. Highly differential expression of the monocarboxylate transporters MCT2 and MCT4 in the developing rat brain. Neuroscience. 2003;122(3):677-88.
58. Bergersen LH, Magistretti PJ, Pellerin L. Selective postsynaptic co-localization of MCT2 with AMPA receptor GluR2/3 subunits at excitatory synapses exhibiting AMPA receptor trafficking. Cerebral Cortex. 2005;15(4):361-70.
59. Tekkök SB, Brown AM, Westenbroek R, Pellerin L, Ransom BR. Transfer of glycogen-derived lactate from astrocytes to axons via specific monocarboxylate transporters supports mouse optic nerve activity. Journal of Neuroscience Research. 2005;81(5):644-52.

60. Bröer S, Bröer A, Schneider HP, Stegen C, Halestrap AP, Deitmer JW. Characterization of the high-affinity monocarboxylate transporter MCT2 in Xenopus laevis oocytes. Biochemical Journal. 1999;341(3):529-35.
61. Bergersen L, Jóhannsson E, Veruki ML, Nagelhus EA, Halestrap A, Sejersted OM, et al. Cellular and subcellular expression of monocarboxylate transporters in the pigment epithelium and retina of the rat. Neuroscience. 1999;90(1):319-31.
62. Rinholm JE, Bergersen LH. White matter lactate – Does it matter? Neuroscience. 2014;276:109-16.
63. Nehlig A, Pereira de Vasconcelos A. Glucose and ketone body utilization by the brain of neonatal rats. Progress in Neurobiology. 1993;40(2):163-220.
64. Wu M, Hernandez M, Shen S, Sabo JK, Kelkar D, Wang J, et al. Differential modulation of the oligodendrocyte transcriptome by sonic hedgehog and bone morphogenetic protein 4 via opposing effects on histone acetylation. Journal of Neuroscience. 2012;32(19):6651-64.
65. Tassinari IDÁ, Andrade MKG, da Rosa LA, Hoff MLM, Nunes RR, Vogt EL, et al. Lactate Administration Reduces Brain Injury and Ameliorates Behavioral Outcomes Following Neonatal Hypoxia–Ischemia. Neuroscience. 2020;448:191-205.
66. Cooper G, . The Cell: A Molecular Approach. 2nd edition. Signaling Molecules and their receptors Sunderland (MA); 2000 [Available from: https://www.ncbi.nlm.nih.gov/books/NBK9924/.
67. Gladden LB. Lactate metabolism: a new paradigm for the third millennium. The Journal of physiology. 2004;558(Pt 1):5-30.
68. Brooks GA. Lactate shuttles in Nature. Biochem Soc T. 2002;30(2):258-64.
69. Hirschhaeuser F, Sattler UGA, Mueller-Klieser W. Lactate: A Metabolic Key Player in Cancer. Cancer Research. 2011;71(22):6921-5.
70. Lauritzen KH, Morland C, Puchades M, Holm-Hansen S, Hagelin EM, Lauritzen F, et al. Lactate Receptor Sites Link Neurotransmission, Neurovascular Coupling, and Brain Energy Metabolism. Cerebral Cortex. 2013;24(10):2784-95.
71. Marchese A, George SR, Kolakowski LF, Lynch KR, O'Dowd BF. Novel GPCRs and their endogenous ligands: expanding the boundaries of physiology and pharmacology. Trends in Pharmacological Sciences. 1999;20(9):370-5.
72. Schöneberg T, Schulz A, Biebermann H, Hermsdorf T, Römpler H, Sangkuhl K. Mutant G-protein-coupled receptors as a cause of human diseases. Pharmacology & Therapeutics. 2004;104(3):173-206.
73. Lee DK, Nguyen T, Lynch KR, Cheng R, Vanti WB, Arkhitko O, et al. Discovery and mapping of ten novel G protein-coupled receptor genes. Gene. 2001;275(1):83-91.
74. Liu C, Wu J, Zhu J, Kuei C, Yu J, Shelton J, et al. Lactate Inhibits Lipolysis in Fat Cells through Activation of an Orphan G-protein-coupled Receptor, GPR81*. J Biol Chem. 2009;284(5):2811-22.
75. Taggart AK, Kero J, Gan X, Cai TQ, Cheng K, Ippolito M, et al. (D)-beta-Hydroxybutyrate inhibits adipocyte lipolysis via the nicotinic acid receptor PUMA-G. J Biol Chem. 2005;280(29):26649-52.
76. Ahmed K, Tunaru S, Langhans C-D, Hanson J, Michalski CW, Kölker S, et al. Deorphanization of GPR109B as a Receptor for the Oxidation Intermediate 3-OH-octanoic Acid and Its Role in the Regulation of Lipolysis J Biol Chem. 2009;284(33):21928-33.
77. Offermanns S, Colletti SL, Lovenberg TW, Semple G, Wise A, IJzerman AP. International Union of Basic and Clinical Pharmacology. LXXXII: Nomenclature and Classification of Hydroxy-carboxylic Acid Receptors (GPR81, GPR109A, and GPR109B). Pharmacological Reviews. 2011;63(2):269-90.
78. Cai TQ, Ren N, Jin L, Cheng K, Kash S, Chen R, et al. Role of GPR81 in lactate-mediated reduction of adipose lipolysis. Biochem Biophys Res Commun. 2008;377(3):987-91.

79. Gantz I, Muraoka A, Yang Y-K, Samuelson LC, Zimmerman EM, Cook H, et al. Cloning and Chromosomal Localization of a Gene (GPR18) Encoding a Novel Seven Transmembrane Receptor Highly Expressed in Spleen and Testis. Genomics. 1997;42(3):462-6.
80. Ge H, Weiszmann J, Reagan JD, Gupte J, Baribault H, Gyuris T, et al. Elucidation of signaling and functional activities of an orphan GPCR, GPR81. J Lipid Res. 2008;49(4):797-803.
81. Rooney K, Trayhurn P. Lactate and the GPR81 receptor in metabolic regulation: implications for adipose tissue function and fatty acid utilisation by muscle during exercise. Br J Nutr. 2011;106(9):1310-6.
82. de Castro Abrantes H, Briquet M, Schmuziger C, Restivo L, Puyal J, Rosenberg N, et al. The Lactate Receptor HCAR1 Modulates Neuronal Network Activity through the Activation of G(α) and G(βγ) Subunits. J Neurosci. 2019;39(23):4422-33.
83. Ahmed K, Tunaru S, Tang C, Müller M, Gille A, Sassmann A, et al. An Autocrine Lactate Loop Mediates Insulin-Dependent Inhibition of Lipolysis through GPR81. Cell Metabolism. 2010;11(4):311-9.
84. Lauritz H. Kennedy ERG, Vuk Palibrk, Marco Pannone, Wei Wang, Ali H.J. Al-Jabri, Rajikala Suganthan, Niklas Meyer, Xiaolin Lin, Linda H. Bergersen, Magnar Bjørås, Johanne E. Rinholm. Lactate receptor HCAR1 regulates neurogenesis and microglia activation after neonatal hypoxia-ischemia. bioRxiv. 2020.
85. Stäubert C, Broom OJ, Nordström A. Hydroxycarboxylic acid receptors are essential for breast cancer cells to control their lipid/fatty acid metabolism. Oncotarget. 2015;6(23):19706-20.
86. Durukan A, Tatlisumak T. Acute ischemic stroke: Overview of major experimental rodent models, pathophysiology, and therapy of focal cerebral ischemia. Pharmacology Biochemistry and Behavior. 2007;87(1):179-97.
87. Krafft PR, Bailey EL, Lekic T, Rolland WB, Altay O, Tang J, et al. Etiology of stroke and choice of models. Int J Stroke. 2012;7(5):398-406.
88. Sherwood CC, Stimpson CD, Raghanti MA, Wildman DE, Uddin M, Grossman LI, et al. Evolution of increased glia-neuron ratios in the human frontal cortex. Proc Natl Acad Sci U S A. 2006;103(37):13606-11.
89. Jickling GC, Sharp FR. Improving the translation of animal ischemic stroke studies to humans. Metab Brain Dis. 2015;30(2):461-7.
90. Festing S, Wilkinson R. The ethics of animal research. Talking Point on the use of animals in scientific research. EMBO Rep. 2007;8(6):526-30.
91. Ethical Guidelines for the Use of Animals in Research The Norwegian National Research ethics committees National Committee for Research Ethics in Science and Technology (NENT); 2019 [Available from: https://www.forskningsetikk.no/en/guidelines/science-and-technology/ethical-guidelines-for-the-use-of-animals-in-research/.
92. Sejersted Y, Hildrestrand GA, Kunke D, Rolseth V, Krokeide SZ, Neurauter CG, et al. Endonuclease VIII-like 3 (Neil3) DNA glycosylase promotes neurogenesis induced by hypoxia-ischemia. Proc Natl Acad Sci U S A. 2011;108(46):18802-7.
93. Koenig H, Groat RA, Windle WF. A Physiological Approach to Perfusion-Flxation of Tissues with Formalin. Stain Technology. 1945;20(1):13-22.
94. Thavarajah R, Mudimbaimannar VK, Elizabeth J, Rao UK, Ranganathan K. Chemical and physical basics of routine formaldehyde fixation. J Oral Maxillofac Pathol. 2012;16(3):400-5.
95. Fix AS, Garman RH. Practical Aspects of Neuropathology: A Technical Guide for Working with the Nervous System. Toxicologic Pathology. 2000;28(1):122-31.
96. Kasukurthi R, Brenner MJ, Moore AM, Moradzadeh A, Ray WZ, Santosa KB, et al. Transcardial perfusion versus immersion fixation for assessment of peripheral nerve regeneration. Journal of Neuroscience Methods. 2009;184(2):303-9.

97. Kiernan JA. Formaldehyde, Formalin, Paraformaldehyde And Glutaraldehyde: What They Are And What They Do. Microscopy Today. 2000;8(1):8-13.
98. Gratzner HG. Monoclonal antibody to 5-bromo- and 5-iododeoxyuridine: A new reagent for detection of DNA replication. Science. 1982;218(4571):474-5.
99. Coons AH, Creech HJ, Jones RN, Berliner E. The demonstration of pneumococcal antigen in tissues by the use of fluorescent antibody. J Immunol. 1942;45(3):159-70.
100. Ramos-Vara JA. Technical Aspects of Immunohistochemistry. Veterinary Pathology. 2005;42(4):405-26.
101. Alberts B, Johnson A, Lewis J, Raff M, Roberts K, Walter P. Molecular biology of the cell, 6th edition Garland Publishing Inc; 2014. 535-46 p.
102. Chen X, Cho D-B, Yang P-C. Double staining immunohistochemistry. N Am J Med Sci. 2010;2(5):241-5.
103. K.R V, Jones D, Udupa V. A simple and effective heat induced antigen retrieval method. MethodsX. 2016;3:315-9.
104. Minsky M. Memoir on inventing the confocal scanning microscope. Scanning. 1988;10(4):128-38.
105. Fellers TJ, Davidson MW. Introduction to Confocal Microscopy Florida Olympus; [Available from: https://www.olympus-lifescience.com/en/microscope-resource/primer/techniques/confocal/confocalintro/.
106. Collins TJ. ImageJ for microscopy. Biotechniques. 2007;43(1 Suppl):25-30.
107. Raster graphics Encyclopaedia Britannica 2020 [Available from: https://www.britannica.com/technology/raster-graphics.
108. Šidák Z. Rectangular Confidence Regions for the Means of Multivariate Normal Distributions. Journal of the American Statistical Association. 1967;62(318):626-33.
109. Mahmood T, Yang P-C. Western blot: technique, theory, and trouble shooting. N Am J Med Sci. 2012;4(9):429-34.
110. Bradford MM. A rapid and sensitive method for the quantitation of microgram quantities of protein utilizing the principle of protein-dye binding. Anal Biochem. 1976;72:248-54.
111. Čepin U. Real-time PCR (qPCR) technology basics Biosistemika.com BioSistemika; 2017 [cited 2021 17.03]. Available from: https://biosistemika.com/blog/qpcr-technology-basics/.
112. Rodríguez-Lázaro D, Hernández M. IDENTIFICATION METHODS | Real-Time PCR. In: Batt CA, Tortorello ML, editors. Encyclopedia of Food Microbiology (Second Edition). Oxford: Academic Press; 2014. p. 344-50.
113. Wagner EM. Monitoring gene expression: quantitative real-time rt-PCR. Methods Mol Biol. 2013;1027:19-45.
114. Wang F, Flanagan J, Su N, Wang L-C, Bui S, Nielson A, et al. RNAscope: A Novel in Situ RNA Analysis Platform for Formalin-Fixed, Paraffin-Embedded Tissues. The Journal of Molecular Diagnostics. 2012;14(1):22-9.
115. Revilla V, Jones A. Cryostat sectioning of brains. International Review of Neurobiology. 47: Academic Press; 2002. p. 61-70.
116. Ahmed K. Biological roles and therapeutic potential of hydroxy-carboxylic Acid receptors. Front Endocrinol (Lausanne). 2011;2:51-.
117. Morland C, Andersson KA, Haugen ØP, Hadzic A, Kleppa L, Gille A, et al. Exercise induces cerebral VEGF and angiogenesis via the lactate receptor HCAR1. Nature Communications. 2017;8(1):15557.
118. BrainMaps. An Interactive Multiresolution Brain Atlas [cited 2021 04.05]. Available from: http://brainmaps.org.

119. Institute of M, National Academy of S, Committee on the Use of Animals in R. Science, Medicine, and Animals: National Academies Press; 1991.
120. Fox JG, Barthold S, Davisson M, Newcomer CE, Quimby FW, Smith A. The mouse in biomedical research: normative biology, husbandry, and models: Elsevier; 2006.
121. Chinwalla AT, Cook LL, Delehaunty KD, Fewell GA, Fulton LA, Fulton RS, et al. Initial sequencing and comparative analysis of the mouse genome. Nature. 2002;420(6915):520-62.
122. Perlman RL. Mouse models of human disease: An evolutionary perspective. Evolution, Medicine, and Public Health. 2016;2016(1):170-6.
123. Vannucci RC, Vannucci SJ. Perinatal Hypoxic-Ischemic Brain Damage: Evolution of an Animal Model. Developmental Neuroscience. 2005;27(2-4):81-6.
124. Crawley JN. Unusual behavioral phenotypes of inbred mouse strains. Trends in Neurosciences. 1996;19(5):181-2.
125. El-Brolosy MA, Stainier DYR. Genetic compensation: A phenomenon in search of mechanisms. PLOS Genetics. 2017;13(7):e1006780.
126. Levine S. Anoxic-ischemic encephalopathy in rats. Am J Pathol. 1960;36(1):1-17.
127. Sheldon RA, Sedik C, Ferriero DM. Strain-related brain injury in neonatal mice subjected to hypoxia–ischemia. Brain Research. 1998;810(1):114-22.
128. Menkes JH, Curran J. Clinical and MR correlates in children with extrapyramidal cerebral palsy. AJNR Am J Neuroradiol. 1994;15(3):451-7.
129. Graham SM, McCullough LD, Murphy SJ. Animal models of ischemic stroke: balancing experimental aims and animal care. Comp Med. 2004;54(5):486-96.
130. Carmichael ST. Rodent models of focal stroke: size, mechanism, and purpose. NeuroRx. 2005;2(3):396-409.
131. Hainsworth AH, Markus HS. Do in vivo experimental models reflect human cerebral small vessel disease? A systematic review. J Cereb Blood Flow Metab. 2008;28(12):1877-91.
132. Scientific TF. RNA quantitation is an important and necessary step prior to most RNA analysis methods [cited 2021 04.05]. Available from: https://www.thermofisher.com/no/en/home/references/ambion-tech-support/rna-isolation/tech-notes/quantitating-rna.html.
133. Shi SR, Key ME, Kalra KL. Antigen retrieval in formalin-fixed, paraffin-embedded tissues: an enhancement method for immunohistochemical staining based on microwave oven heating of tissue sections. Journal of Histochemistry & Cytochemistry. 1991;39(6):741-8.
134. Prasad SS, Russell M, Nowakowska M, Williams A, Yauk C. Gene Expression Analysis to Identify Molecular Correlates of Pre- and Post-conditioning Derived Neuroprotection. Journal of Molecular Neuroscience. 2012;47(2):322-39.
135. Wen Y, Yang S, Liu R, Simpkins JW. Cell-cycle regulators are involved in transient cerebral ischemia induced neuronal apoptosis in female rats. FEBS Letters. 2005;579(21):4591-9.
136. Lambertus M, Øverberg LT, Andersson KA, Hjelden MS, Hadzic A, Haugen ØP, et al. L-lactate induces neurogenesis in the mouse ventricular-subventricular zone via the lactate receptor HCA1. Acta Physiologica. 2021;231(3):e13587.
137. Wu Y, Wang M, Zhang K, Li Y, Xu M, Tang S, et al. Lactate enhanced the effect of parathyroid hormone on osteoblast differentiation via GPR81-PKC-Akt signaling. Biochemical and Biophysical Research Communications. 2018;503(2):737-43.
138. Roelants-Van Rijn AM, van der Grond J, de Vries LS, Groenendaal F. Value of (1)H-MRS using different echo times in neonates with cerebral hypoxia-ischemia. Pediatr Res. 2001;49(3):356-62.

139. Zheng Y, Wang X-M. Measurement of Lactate Content and Amide Proton Transfer Values in the Basal Ganglia of a Neonatal Piglet Hypoxic-Ischemic Brain Injury Model Using MRI. American Journal of Neuroradiology. 2017;38(4):827-34.
140. Hadzic A, Nguyen TD, Hosoyamada M, Tomioka NH, Bergersen LH, Storm-Mathisen J, et al. The Lactate Receptor HCA(1) Is Present in the Choroid Plexus, the Tela Choroidea, and the Neuroepithelial Lining of the Dorsal Part of the Third Ventricle. Int J Mol Sci. 2020;21(18).

8. Appendix

Section A

Reagents, kits, consumables, instruments, and software.

Table A1. Reagents, producers, and catalogue numbers

Reagent	Producer	Catalogue nr:
Normal goat serum (NGS)	Sigma-Aldrich®, Darmstadt, Germany	69023
Bovine serum albumin (BSA) Cohn fraction V, protease free	Saween & Werner, Limhamn, Sweden	B2000-500
Phosphate-buffered saline (PBS)	Oslo Universitetssykehus, avdeling for mikrobiologi	-
ProLong™ Glass Antifade Mountant	Thermo Fisher Scientific, Waltham, MA, USA	P36930
Triton™ X-100	Sigma-Aldrich®, Darmstadt, Germany	T8787
10x Tris/Glycine/SDS buffer	Bio-Rad Laboratories, Hercules, CA, USA	161-0772
Skim Milk Powder	Sigma-Aldrich®, Darmstadt, Germany	70166
DAPI for nucleic acid staining	Sigma-Aldrich®, Darmstadt, Germany	D9542
0.5M EDTA Solution (100X)	Thermo Fisher Scientific, Waltham, MA, USA	1861274
Halt™ Protease and Phosphatase Inhibitor Single-Use Cocktail (100X)	Thermo Fisher Scientific, Waltham, MA, USA	78442
SuperSignal™ West Femto Luminol/ Enhancer Solution	Thermo Fisher Scientific, Waltham, MA, USA	1856189
SuperSignal™ West Femto Stable Peroxide Buffer	Thermo Fisher Scientific, Waltham, MA, USA	1856190
NuPAGE® LDS sample buffer (4X)	Thermo Fisher Scientific, Waltham, MA, USA	NP0008
Power SYBR™ Green PCR Master Mix	Thermo Fisher Scientific, Waltham, MA, USA	4367659
Opal™ 540 Reagent Pack	AKOYA Biosciences Marlborough, MA, USA	FP1494001KT
TWEEN® 20	Sigma-Aldrich®, Darmstadt, German	P1379
Paraformaldehyde solution 4% in PBS,	Santa Cruz Biotechnology, TX, USA	sc-281692
10% Neutral Buffered Formalin	Sigma-Aldrich®, Darmstadt, German	HT501128-4L
RNAscope® Probe- Mm-HCAR1/Gpr81, Target region: 886 – 1758	ACD Bio, Newark, CA, USA	317421

Table A2. Kits, producers, and catalogue numbers

Kit	Producer	Catalogue nr.
SuperSignal™ West Femto Maximum sensitivity substrate	Thermo Fisher Scientific, Waltham, MA, USA	34095
RNeasy Plus Mini Kit	QIAGEN, Hilden, Germany	72134
High-Capacity cDNA Reverse Transcription Kit	Thermo Fisher Scientific, Waltham, MA, USA	4368814
RNAscope® Multiplex Fluorescent Reagents Kit v2	ACD Bio Newark, CA, USA	323100
RNA-Protein Co-Detection Ancillary Kit	ACD Bio Newark, CA, USA	323180

Table A3. Consumables, producers, and catalogue nr.

Consumables	Producer	Catalogue nr.
12% Mini-PROTEAN® TGX™ Precast Protein Gel	Bio-Rad Laboratories, Hercules, CA, USA	4561045
Trans-Blot® Turbo™ Mini PVDF Membrane, 0.2 µm	Bio-Rad Laboratories, Hercules, CA, USA	1704156
Precision Plus Protein™ Dual Color Standards	Bio-Rad Laboratories, Hercules, CA, USA	1610374
Protein Assay Dye Reagent Concentrate	Bio-Rad Laboratories, Hercules, CA, USA	5000006
Richard-Allan Scientific Clear-Rite™	Thermo Fisher Scientific, Waltham, MA, USA	22-046341
Superfrost™ Microscope Slides	Thermo Fisher Scientific, Waltham, MA, USA	12372098
Menzel™ Microscope Coverslips	Thermo Fisher Scientific, Waltham, MA, USA	11778691
Absolutt alkohol prima ren	Antibac, Asker, Norge	600068
Carl Zeiss™ Immersol™ Immersion Oil	Thermo Fisher Scientific, Waltham, MA, USA	10539438
QIAshredder	QIAGEN, Hilden, Germany	79656
Fisherbrand™ RNase-Free Disposable Pellet Pestles	DWK Life Sciences, LLC, NJ, USA	12141364
MicroAmp® Fast 96-well Reaction Plate	Thermo Fisher Scientific, Waltham, MA, USA	4346907
MicroAmp™ Optical Adhesive Film	Thermo Fisher Scientific, Waltham, MA, USA	4360954
Epredia™ Neg-50™ Frozen Section Medium	Thermo Fisher Scientific, Waltham, MA, USA	11912365
Thermo Scientific™ Ultra Disposable Microtome Blades	Thermo Fisher Scientific, Waltham, MA, USA	3053835
ImmEDGE™ Hydrophobic Barrier Pen	Thermo Fisher Scientific, Waltham, MA, USA	NC9545623

Table A4. Equipment and instruments, producer, and catalogue nr.

Equipment and instruments	Producer	Catalogue nr.
Leica TCS SP8 gSTED microscopy	Leica Microsystems, Santa Clara, CA, USA	-
Trans-Blot® Turbo™ Transfer System	Bio-Rad Laboratories, Hercules, CA, USA	1704150EDU
XCell SureLock Mini-Cell™	Thermo Fisher Scientific, Waltham, MA, USA	EI0001
Microcentrifuge 5424 R	Eppendorf®, Hamburg, Germany	Z722960
MegaFuge 1.0R refrigerated centrifuge	Heraeus Instruments	LV40799952
Microm HM355S Rotary Microtome	Thermo Fisher Scientific, Waltham, MA, USA	905200ER
Thermo Scientific™ Section Transfer System™	Thermo Fisher Scientific, Waltham, MA, USA	771200
Termaks 24L Heating incubator	Termarks AS, Bergen, Norway	390-0750NO
Immuno slide staining tray (moisture chamber)	Pyramid Innovation, Polegate, England	R64001-E
Applied Biosystems™ 2720 Thermal Cycler	Thermo Fisher Scientific, Waltham, MA, USA	12313653
Bio-rad ChemiDoc™ MP system	Bio-Rad Laboratories, Hercules, CA, USA	1708280
PELLET PESTLE® Cordless Motor	DWK Life Sciences, LLC, NJ, USA	749540
LABINCO L201 Rock'n Roller	Labinco BV, DG Breda, The Netherlands	20100
StepOnePlus™ Real-Time PCR System.	Thermo Fisher Scientific, Waltham, MA, USA	4376600
NanoDrop™ Spectrophotometer	Thermo Fisher Scientific, Waltham, MA, USA	13400518
Microplate centrifuge, PCR Plate Spinner	VWR International AS Bergen, Norway	5211648
CryoStar™ NX70 Cryostat	Thermo Fisher Scientific, Waltham, MA, USA	957000L
HybEZ™ II Hybridization system	ACD Bio, Newark, CA, USA	321721
HybEZ™ Humidity Control Tray with lid	ACD Bio, Newark, CA, USA	310012
RNAscope® EZ-Batch™ Slide Rack with wash tray	ACD Bio, Newark, CA, USA	310017
HybEZ™ Humidifying paper	ACD Bio, Newark, CA, USA	310015

Table A5. Software and developers

Software	Developer
Fiji, Image J	Rasband, National Institutes of Health (NIH), Maryland, USA
LASX software	Leica Microsystems, Santa Clara, CA, USA
ImageLab	Bio-Rad Laboratories, Hercules, CA, USA
Microsoft® Excel	Microsoft, Redmond, WA, USA
GraphPad, Prism	GraphPad Software by Dr. Harvey Motulsky, San Diego, CA, USA

Section B

Table B1. Antibody, host, dilution, producer, and catalogue nr.

Antibody	Host	Dilution	Producer	Catalogue nr.
Olig2	Rabbit	1:200	Merck Millipore	MAB9610
BrdU	Rat	1.200	Abcam	AB6326
APC	Mouse	1:100	Abcam	AB16794
ß-Actin	Mouse	1:2000	Abcam	AB8227
Alexa Fluor 488 anti-rabbit	Goat	1:400	Invitrogen	A11034
Alexa Fluor 633 anti-rat	Goat	1:400	Invitrogen	A21094
Alexa Fluor 555 anti-mouse	Goat	1:400	Invitrogen	A21424
HRP-labelled Anti-rabbit	Goat	1:20000	EpiGentek	C10018-1
HRP-labelled Anti mouse	Donkey	1:10000	Abcam	AB6820

Table B2. Reagents and volume per reaction in synthesis of cDNA.

Reagent	Volume
10 X Reverse Transcription buffer	2 µL
25 X deoxynucleotide triphosphate mix	0.8 µL
10 X Random primers	2 µL
Reverse Transcriptase	1 µL
RNAse free H_2O	4.2 µL
Total RNA 200ng/ µL	10 µL
Total	20 µL

Table B3. cDNA reverse transcription reaction conditions

Temperature profile	Time profile
25 °C	10 minutes
37 °C	2 hours
85 °C	5 minutes
4 °C	∞

Table B4. RT-qPCR mixture reagents and volume per reaction

PCR reaction reagent	Volume/reaction
PowerUp™ SYBR™ Green Master Mix	10 µL
RNAse free H_2O	6 µL
Forward primer	2 µL
Reverse primer	2 µL
Sample cDNA (1:10)	2 µL
Total	20 µL

Table B5. RT-qPCR reaction conditions.

Temperature profile	Time profile
95 °C	10 min
95 °C	15 sec x 40
60 °C	1 min x 40
95 °C	15 sec
60 °C	1 min
95 °C	15 sec

Genotyping of WT and HCAR1 KO mice.

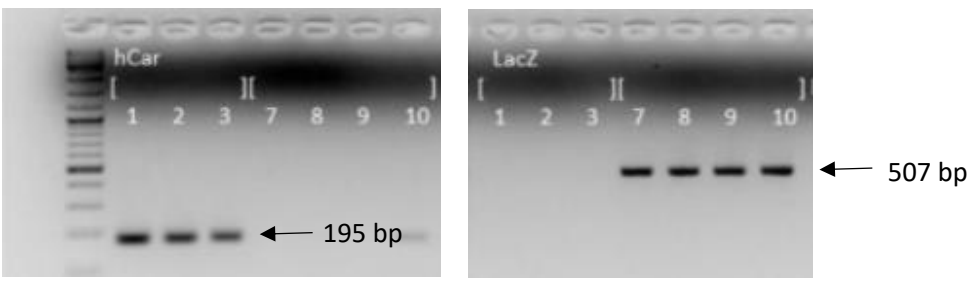

Genotypes were determined by polymerase chain reaction (PCR) followed by agarose gel electrophoresis of DNA samples extracted from mouse ears. In the HCAR1 KO, the gene is exchanged with a cassette encoding β-galactosidase (LacZ) and neomycin-resistance. WT was confirmed with a clear band for HCAR1 (195 bp) and HCAR1 KO was confirmed with a clear band for LacZ (507 bp). Examples from the genotyping is illustrated above. WT mice (1-3) show a clear band at 195 bp, while KO mice (7-10) show a clear band at 507 bp.

Section C
Solutions and buffers

PBS (0.01 M, pH 7.4)

Citrate buffer (10 mM, pH 6.0)

Block solution IHC

- 10% Normal goat serum
- 1% Bovine serum albumin
- 0,5 % Triton X-100
- Diluted in PBS

Primary and secondary antibody solution:

- 3 % NGS
- 1 % BSA
- 0,5 % Triton X-100
- Diluted in PBS

1x Tris/Glycine/SDS buffer/Running buffer

- 100 mL 10 x Tris/Glycine/SDS buffer
- 900 mL MQ –H_2O

Final concentration 1x solution, pH 8.3:

- 25 mM Tris
- 192 mM Glycine
- 0.1% (w/v) SDS

Block solution Western blotting

- 5 % Skim milk powder
- Diluted in PBS-T

Phosphate Buffered Saline with Tween 20 (PBS-T) pH 7.4

- NaCl: 137 mM
- KCl: 2.7 mM
- Na_2HPO_4: 10 mM
- KH_2PO_4: 1.8 mM
- Tween® 20 detergent: 0.1% (w/v)

Norges miljø- og biovitenskapelige universitet
Noregs miljø- og biovitskapelege universitet
Norwegian University of Life Sciences

Postboks 5003
NO-1432 Ås
Norway